TAE 2022 - Cosmology Notes

David Alonso – University of Oxford

August 30, 2022

Abstract

These notes are a summary of the material covered in the 2022 Taller de Altas Energias cosmology course, and are meant to be a companion for those lectures. The course consists of three 1-hour lectures and a 1-hour tutorial covering a few specific calculations. This is obviously a very short amount of time in which to cover all relevant theoretical aspects of modern cosmology, and thus the material is limited in scope. I have aimed to cover the basics of cosmological background, perturbation theory, inflation, structure formation, CMB physics, and weak gravitational lensing. In spite of missing a wide range of important topics (e.g. reheating, Big-Bang nucleosynthesis, tensor perturbations, CMB polarization, non-linear structure formation models, data analysis methods), this is already a very ambitious syllabus for just three hours! Therefore, I have often provided results without a thorough derivation, or which hold only under specific assumptions that must be dropped in real-life calculations. Those interested in delving deeper into cosmological theory should therefore work through the details I have only skimmed, making use of existing textbooks as well as the primary literature that set the foundations of modern cosmology. Where possible, I have provided references to these materials. As an example, the notes themselves are heavily based on [1, 2, 3].

Contents

1 Homogeneous cosmology

References

For more information on background cosmology, refer to [2, 4, 5].

1.1 The Copernican principle and FRW

Much of modern cosmology is based on the so-called "Cosmological principle", related to the Copernican principle:

> *On large enough scales, the Universe is homogeneous and isotropic.*

In mathematical terms, this implies that the metric describing the large-scale Universe is given by a set of maximally-symmetric constant-time slices. The most general version of such a metric is[1]:

$$d\tau^2 = b^2(t)dt^2 - a^2(t)S_{ij}dx^i dx^j, \tag{1}$$

where b and a are functions of time only, and S_{ij} is a maximally-symmetric 3D metric (i.e. a space-like metric with 6 Killing vectors). Maximally symmetric spaces can be classified in terms of a single curvature parameter k as "closed" ($k > 0$), "open" ($k < 0$), or "flat" ($k = 0$). The metric in this case takes the general form:

$$S_{ij}dx^i dx^j = d\chi^2 + \mathrm{sinn}^2(\chi)\left[d\theta^2 + \sin^2(\theta)d\varphi^2\right], \tag{2}$$

where

$$\mathrm{sinn}(\chi) = \begin{cases} k^{-1/2}\sin(\sqrt{k}\chi) & k > 0 \\ \chi & k = 0 \\ |k|^{-1/2}\sinh(\sqrt{-k}\chi) & k < 0 \end{cases} \tag{3}$$

Since most observational evidence seems to be compatible with a flat Universe, for simplicity we well assume from here on that $k = 0$ unless otherwise stated.

To simplify things further, we will make use of "comoving coordinates" to describe the system. These are defined as follows: consider a space-filling fluid. At some point in time, we assign a label (3-dimensional coordinates) to each fluid element, and we synchronise the imaginary clocks carried by each element. Then, we define the coordinates of any event in spacetime by assigning it, as spatial coordinates, the label of the fluid element it occupies, and as time coordinate, the time measured by the element's clock. In this case, since t is the time measured by a comoving observer (for whom the spatial coordinates are constant), the function $b(t)$ must be $b(t) = 1$. Thus defined, t is usually called "cosmic time".

Under these assumptions, the metric takes the simple form (depending on whether you choose to use spherical or Cartesian coordinates:

$$d\tau^2 = dt^2 - a^2(t)\left[d\chi^2 + \chi^2(d\theta^2 + \sin^2\theta\, d\varphi^2)\right] = dt^2 - a^2(t)|d\mathbf{x}|^2. \tag{4}$$

This is the flat version of the so-called Friedmann-Robertson-Walker (FRW) metric. It will sometimes be useful to use "conformal time" η, defined as $a\, d\eta = dt$, in which case the metric is conformally Minkowski:

$$d\tau^2 = a^2(\eta)\left(d\eta^2 - |d\mathbf{x}|^2\right). \tag{5}$$

The function $a(t)$ is the so-called *scale factor*, and it reflects the "size" of the Universe with respect to the time t_0 when the comoving fluid elements were assigned their labels. It is common in cosmology to assign t_0 to the current time, so that $a(t_0) = 1$ today.

1.2 The geodesic equation and redshift

Since most or all of our data in cosmology come from elecromagnetic radiation from various sources, studying the propagation of photons in an expanding background is of crucial importance.

Consider a photon propagating radially towards (or from) the observer sitting at $\chi = 0$. The geodesic equation for the t coordinate reads, after fixing θ and φ:

$$\frac{dp^t}{d\lambda}\left(\frac{dt}{d\lambda}\right) = -a\dot{a}\,(p^\chi)^2, \tag{6}$$

where λ is an affine parameter, $\dot{a} \equiv da/dt$, and we have defined the time component of the photon 4-momentum $p^t \equiv dt/d\lambda$ and its radial component $p^\chi \equiv d\chi/d\lambda$. Likewise, the condition $d\tau^2 = 0$ implies $(p^t)^2 = a^2\,(p^\chi)^2$. Using this to substitute p^χ in the previous equation we obtain

$$\frac{dp^t}{d\lambda} = -Hp^t\frac{dt}{d\lambda}, \tag{7}$$

where we have defined the *expansion rate*:

$$H \equiv \frac{\dot{a}}{a}. \tag{8}$$

[1] A beautiful and thorough proof of this can be found in [5].

Integrating Eq. 7 we obtain the simple result

$$p^t \propto a^{-1}. \tag{9}$$

Thus, since the photon frequency measured by a comoving observer is $\nu \propto p^t$, photons are redshifted (or blueshifted if $a(t)$ is a decreasing function) as they propagate. Defining the redshift z as the shift in the wavelength of a photon observed today with respect to the rest-frame wavelength at the comoving emitter

$$z \equiv \frac{\lambda - \lambda_{\rm em}}{\lambda_{\rm em}}, \tag{10}$$

Eq. 9 can be rewritten as a relation between scale factor and redshift

$$a(t) = \frac{1}{1+z}. \tag{11}$$

As we will see, t, η, a, and z are used in different contexts as time labels.

1.3 Distances

Distances to objects in the FRW metric can be calculated in different ways, more or less connected with actual observations.

- **Comoving distance.** Consider a comoving source emitting photons at time t_E from coordinate χ_E, corresponding to redshift z, reaching us at t_0 having propagated radially. Using the line element for photons, the radial distance is

$$\chi = \int_0^{\chi_E} d\chi = \int_{t_E}^{t_0} \frac{dt}{a}. \tag{12}$$

  Changing the integration variable to redshift, yields:

$$\chi(z) = \int_0^z \frac{dz'}{H(z')}. \tag{13}$$

- **Proper radial distance.** Consider a set of comoving observers lying on a straight line between us and a comoving source at χ_E. At a fixed cosmic time t all observers measure the distance to the next by sending a photon to it and back, and measuring the corresponding time interval $d\ell = dt$. Adding up the contributions from all observers:

$$d(\text{distance}) = dt = a(t)d\chi. \tag{14}$$

  Integrating over χ yields the proper physical radial distance:

$$d_p = a(t)\chi. \tag{15}$$

- **Angular diameter distance.** Consider an extended object at redshift z of size $\Delta\ell$, and subtending an angle $\Delta\theta$. The angular diameter distance is defined as $d_A \equiv \Delta\ell/\Delta\theta$. Using the FRW metric, $\Delta\ell = \chi(z)\Delta\theta/(1+z)$, and therefore

$$d_A(z) = \frac{\chi(z)}{1+z}. \tag{16}$$

- **Luminosity distance.** The luminosity distance d_L to an object of rest-frame luminosity L at redshift z, and measured flux F is defined as:

$$F = \frac{L}{4\pi d_L^2}. \tag{17}$$

  The luminosity is the amount of energy emitted per unit time $L \equiv dE_E/dt_E$, both measured at the emitter's frame. Due to the expansion, the photon energies are redshifted ($dE_O = dE_E/(1+$

z). The expansion also stretches the arrival time between photons, so that $dt_O = (1+z)dt_E$. Finally, all the emitted energy is spread over an area $4\pi\chi^2$ by the time it reaches the observer at $z = 0$. The measured flux (energy per unit time and detector area) is then

$$F = \frac{L}{4\pi((1+z)\chi)^2}, \tag{18}$$

and therefore the luminosity distance is

$$d_L(z) = (1+z)\chi(z). \tag{19}$$

The relation between angular and luminosity distances $d_L(z) = (1+z)^2 d_A(z)$ is the so-called *Etherington relation*, and actually holds in any metric theory of gravity (not just FRW).

- **Particle horizon.** The (comoving) particle horizon is the largest (comoving) distance covered by a photon emitted at the initial singularity (i.e. $z = \infty$). Following the rationale above, the horizon at redshift z is

$$d_H(z) = \int_z^\infty \frac{dz'}{H(z')} = \chi_\infty - \chi(z). \tag{20}$$

Often $d_H \sim (aH)^{-1}$, up to a factor of $\mathcal{O}(1)$, and therefore $(aH)^{-1}$ is often used as an approximation for the size of the horizon.

1.4 Einstein equations, cosmological parameters

Let's now work out the dynamics of the FRW metric. The first step is deriving the corresponding Einstein equations.

The main components that make up the energy content of the Universe can be treated as perfect fluids. In this case, the energy-momentum tensor is:

$$T_{\mu\nu} = (\rho + p)U_\mu U_\nu - p g_{\mu\nu}, \tag{21}$$

where ρ and p are the energy density and pressure, and U_μ is the fluid's 4-velocity. In comoving coordinates $U_\mu \propto (1,0,0,0)$, and we obtain

$$T^\mu_\nu = \mathrm{diag}(\rho, -p, -p, -p). \tag{22}$$

We will assume the fluid to be made up of several components $T_{\mu\nu} = \sum_i T^i_{\mu\nu}$, and that, for each of these, pressure and energy density are related via a simple equation of state of the form

$$p_i = w_i \rho_i, \tag{23}$$

where w_i is the "equation of state parameter" for the i-th component. Two important such species are non-relativistic matter (sometimes called "dust"), for which $w_M = 0$ (presureless fluid), and relativistic matter or radiation, for which $w_R = 1/3$.

Energy-momentum conservation ($\nabla_\nu T^{\mu\nu} = 0$) holds for each non-interacting component separately. In the FRW case this implies:

$$\dot{\rho}_i + 3H(\rho_i + p_i) = 0. \tag{24}$$

This can be integrated to give the evolution of different species

$$\rho(a) = \rho_0 \exp\left[3\int_a^1 \frac{da'}{a}(1+w)\right] = \rho_0\, a^{-3(1+w)}, \tag{25}$$

where we have assumed w = constant in the second equality. Thus, for matter $\rho_M = \rho_{M,0} a^3$, for radiation $\rho_R = \rho_{R,0} a^4$ and, since for a cosmological constant $\rho_\Lambda = $ const., the equation of state for vacuum energy / Λ is $w_\Lambda = -1$. A departure from $w_\Lambda = -1$ would be a sign that dark energy is more complex than a simple cosmological constant. For this reason, this parameter has become central enough in the search for dark energy that it is often simply called "the equation of state" or w.

Replacing the perfect-fluid $T_{\mu\nu}$ in Einstein's equations leads to the following two independent *Friedmann equations*:

$$H^2 = \frac{8\pi G}{3}\rho - \frac{k}{a^2}, \tag{26}$$

$$\frac{\ddot{a}}{a} = -\frac{4\pi G}{3}(\rho + 3p), \tag{27}$$

where we have brought back curvature for completeness. Note, from the second equation, that any species with an equation of state $w < -1/3$ will contribute to a *positive acceleration*.

Equation 26 motivates defining the cosmological density parameters Ω_i as follows:

$$\Omega_i \equiv \frac{\rho_{i,0}}{\rho_c}, \quad \Omega_k = -\frac{k}{H_0^2} \quad \rho_c \equiv \frac{3H_0^2}{8\pi G}, \tag{28}$$

where ρ_c is the so-called *critical density* today, and the subscript $_0$ denotes quantities evaluated at the present time. It is sometimes convenient to make use of the cosmological parameters evaluated at a different time $a \neq 1$. In those cases, we will make the time-dependence of the parameters explicit (e.g. $\Omega_i(a)$).

Note that the two Friedmann equations are not independent of the energy conservation equation (Eq. 24). Only two of these three equations are independent. Using the solution in Eq. 25, we obtain a compact form for the first Friedmann equation:

$$H^2 = H_0^2 \sum_i \Omega_i \, a^{-3(1+w_i)}, \tag{29}$$

where $w_k \equiv -1/3$.

When a single component dominates the expansion rate, the solution to this equation is

$$a \propto t^{\frac{2}{3(1+w)}}, \quad \text{or} \quad a \propto e^{Ht} \ \text{ for } w = -1. \tag{30}$$

Current observations from CMB, supernovae and galaxy surveys point to the following values for the cosmological parameters:

$$\Omega_k \lesssim 10^{-3}, \quad \Omega_R \sim 8 \times 10^{-5}, \quad \Omega_M \sim 0.3, \quad \Omega_\Lambda \sim 0.7, \quad H_0 \sim 70\,\mathrm{km/s/Mpc}. \tag{31}$$

Thus, at early times the Universe underwent a radiation-dominated phase with $a \propto t^{1/2}$, the expansion slowed down later, during matter domination, to $a \propto t^{2/3}$, and is currently accelerating towards exponential expansion during Λ domination. The redshifts at which the transitions between radiation and matter domination, and matter and Λ domination take place are approximately

$$z_{R\to M} \sim 3000, \quad z_{M\to\Lambda} \sim 0.3. \tag{32}$$

2 Inhomogeneities: The Newtonian treatment

Even though the standard cosmological model is based on the premise that the Universe is homogeneous and isotropic on large scales, it is evident to anyone who has ever looked at the sky at night that it is not so on smaller scales. Structures with very different sizes can be found, from stars and planets at the AU scale ($\sim 4\mu$pc) to galaxies at the kpc scale and clusters and superclusters of galaxies at the Mpc scale. As we will see, these structures have their origin in small linear perturbations at early times in an otherwise homogeneous Universe, which have grown to reach their present non-linear state via gravitational collapse. The theory of inflation gives a fairly satisfactory explanation for the origin of these perturbations in terms of quantum fluctuations in the primordial density field, while the theory of cosmological perturbations and large scale structure studies and models their evolution throughout the history of the Universe.

The evolution of density fluctuations in a cosmological background is a rich topic, and in fact most of cosmological science today focuses on extracting fundamental physics constraints by studying inhomogeneities, rather than the background expansion directly. This is because, for instance, the background expansion affects the way in which structures grow over time. The inhomogeneities

we observe today also contain information about the primordial fluctuations that seeded them, and therefore can advance our understanding of the very early Universe. Furthermore, the statistics of the anisotropies in the Cosmic Microwave Background (CMB) can be used to place very tight constraints on the components that made up the Universe at early times. Finally, the way structure forms and evolves on large scales plays a central role in the formation and evolution of galaxies, and thus a good understanding of structure formation is important for astrophysics too.

References

For more information on Newtonian perturbation theory and structure formation at late times, refer to [1, 2, 6, 7, 8].

2.1 Newtonian perturbations

We will consider a simplified scenario to begin our study of structure formation. We model the density of non-relativistic matter in the Universe as a fluid with density fluctuations around the mean evolving in an expanding background. Although simplified, this treatment turns out to work very well in many regimes of interest in cosmology, particularly at late times, when matter and dark energy dominate the expansion. A more sophisticated, fully-relativistic treatment of perturbations (which we will turn to in Section 3) is necessary if:

- Studying perturbation in a relativistic fluid.
- Studying perturbations on horizon-sized scales $1/\ell \sim H$.

The evolution of a fluid with density $\rho(\mathbf{r}, t)$ and velocity field $\mathbf{V}(\mathbf{r}, t)$ under gravity is governed by three equations:

- The **continuity equation**, which states the conservation of mass:

$$\partial_t \rho + \nabla_{\mathbf{r}} \cdot (\rho \, \mathbf{V}) = 0. \tag{33}$$

- The **Euler equation**, following from Newton's second law:

$$\partial_t \mathbf{V} + (\mathbf{V} \cdot \nabla_{\mathbf{r}})\mathbf{V} + \frac{\nabla_{\mathbf{r}} p}{\rho} + \nabla_{\mathbf{r}} \Psi = 0, \tag{34}$$

  where p and Ψ are the pressure and gravitational potential respectively.

- The **Poisson equation**, stating the connection between matter density and gravity:

$$\nabla^2_{\mathbf{r}} \Psi = 4\pi G \rho. \tag{35}$$

It is useful to note that the continuity and Euler equations can be derived from moments of the collisionless Boltzmann equation (or the Liouville theorem):

$$\frac{\partial f}{\partial t} + \mathbf{V} \cdot \frac{\partial f}{\partial \mathbf{r}} + \dot{\mathbf{p}} \cdot \frac{\partial f}{\partial \mathbf{p}} = 0, \tag{36}$$

where $f(t, \mathbf{r}, \mathbf{p})$ is the phase-space distribution of fluid particles.

Consider now an expanding background, in which the physical coordinates $\mathbf{r}$ are related to Lagrangian coordinates $\mathbf{x}$ (comoving with the background expansion) via $\mathbf{r} = a(t)\,\mathbf{x}$. In this case, the derivatives with respect to $\mathbf{x}$ or $\mathbf{r}$ are related via:

$$\nabla_{\mathbf{r}} = \frac{1}{a} \nabla_{\mathbf{x}}, \quad \partial_t|_{\mathbf{r}} = \partial_t|_{\mathbf{x}} - H\mathbf{x} \cdot \nabla_{\mathbf{x}}. \tag{37}$$

Let's also split ρ, $\mathbf{V}$, Ψ and p into background and perturbations:

$$\rho(t, \mathbf{x}) = \bar{\rho}(t)[1 + \delta(\mathbf{x}, t)], \quad \mathbf{V} = \dot{a}\mathbf{x} + \mathbf{v}, \quad \Psi = \bar{\Psi} + \psi(\mathbf{x}, t), \quad p = \bar{p}(t) + c_s^2 \bar{\rho}(t)\delta(\mathbf{x}, t), \tag{38}$$

which defines the overdensity δ and the peculiar velocity $\mathbf{v}$ and potential ψ. c_s is the sound speed, defined as $c_s^2 \equiv \partial p/\partial\rho$. It is worth noting that, in order to ensure that the background components satisfy the continuity, Euler and Poisson equations, the background potential must be set to

$$\bar{\Psi} = -\frac{1}{2}a\ddot{a}|\mathbf{x}|^2. \tag{39}$$

Substituting these in Eqs. 33, 34 and 35 we obtain the perturbation equations:

$$\dot{\delta} + \frac{1}{a}\nabla\cdot((1+\delta)\mathbf{v}) = 0 \tag{40}$$

$$\dot{\mathbf{v}} + H\mathbf{v} + \frac{1}{a}(\mathbf{v}\cdot\nabla)\mathbf{v} + \frac{c_s^2}{a}\frac{\nabla\delta}{1+\delta} + \frac{1}{a}\nabla\psi = 0 \tag{41}$$

$$\nabla^2\psi = 4\pi G a^2\bar{\rho}\delta, \tag{42}$$

where we abbreviate $\nabla \equiv \nabla_{\mathbf{x}}$.

2.2 Linear theory

Linealising the previous set of equations we obtain

$$\dot{\delta} + \frac{1}{a}\nabla\cdot\mathbf{v} = 0 \tag{43}$$

$$\dot{\mathbf{v}} + H\mathbf{v} + \frac{c_s^2}{a}\nabla\delta + \frac{1}{a}\nabla\psi = 0 \tag{44}$$

$$\nabla^2\psi = 4\pi G a^2\bar{\rho}\delta. \tag{45}$$

Let us define Fourier transform of a field f as:

$$f_{\mathbf{k}}(t) \equiv \int d^3x\, e^{-i\mathbf{k}\cdot\mathbf{x}} f(\mathbf{x},t), \qquad f(\mathbf{x},t) = \int \frac{d^3k}{(2\pi)^3} e^{i\mathbf{k}\cdot\mathbf{x}} f_{\mathbf{k}}(t). \tag{46}$$

The three equations above can then be written in terms of the Fourier transforms of all fields involved as

$$\dot{\delta}_{\mathbf{k}} + \frac{i}{a}\mathbf{k}\cdot\mathbf{v}_{\mathbf{k}} = 0 \tag{47}$$

$$\dot{\mathbf{v}}_{\mathbf{k}} + H\mathbf{v}_{\mathbf{k}} + \frac{i}{a}\mathbf{k}\left[c_s^2\delta_{\mathbf{k}} + \psi_{\mathbf{k}}\right] = 0 \tag{48}$$

$$k^2\psi_{\mathbf{k}} = -4\pi G a^2\bar{\rho}\delta_{\mathbf{k}}. \tag{49}$$

2.2.1 Vorticity

Let us decompose the velocity field $\mathbf{v}_{\mathbf{k}}$ into components parallel and perpendicular to the wavevector $\mathbf{k}$:

$$\mathbf{v}_{\mathbf{k}} = v_{\parallel}\frac{\mathbf{k}}{k} + \mathbf{v}_{\mathbf{k},\perp}, \tag{50}$$

where

$$v_{\parallel} \equiv \frac{\mathbf{v}\cdot\mathbf{k}}{k}, \qquad \mathbf{v}_{\mathbf{k},\perp} \equiv \left(\mathbb{1} - \frac{\mathbf{k}\,\mathbf{k}^T}{k^2}\right)\mathbf{v}_{\mathbf{k}}. \tag{51}$$

Projecting Eq. 48 on the plane perpendicular to $\mathbf{k}$, we obtain

$$\dot{\mathbf{v}}_{\mathbf{k},\perp} + H\mathbf{v}_{\mathbf{k},\perp} = 0, \tag{52}$$

with an immediate solution

$$\mathbf{v}_{\mathbf{k},\perp} \propto \frac{1}{a}. \tag{53}$$

Thus, at linear level, vorticity is a purely decaying mode. Vorticity can only be generated via non-linear evolution (through the third term in Eq. 41), or if sourced by viscosity-like terms (which we have ignored here).

2.2.2 The Jeans equation

We will hereafter consider only the longitudinal velocity component. Taking the divergence of Eq. 48, and substituting in the Poisson equation, we obtain a pair of coupled equations:

$$\dot{\delta}_{\mathbf{k}} + \frac{1}{a}\theta_{\mathbf{k}} = 0 \tag{54}$$

$$\dot{\theta}_{\mathbf{k}} + H\theta_{\mathbf{k}} + \frac{1}{a}\left[4\pi G a^2 \bar{\rho} - c_s^2 k^2\right]\delta_{\mathbf{k}} = 0 \tag{55}$$

These can be combined into a second-order equation for $\delta_{\mathbf{k}}$:

$$\ddot{\delta}_{\mathbf{k}} + 2H\dot{\delta}_{\mathbf{k}} + \left(\frac{c_s^2 k^2}{a^2} - 4\pi G\bar{\rho}\right)\delta = 0. \tag{56}$$

The second term, caused by the background expansion, acts as a friction-like term, slowing down structure growth (which would otherwise be exponential). The third term displays a competition between pressure and gravity.

On small scales, $k \gg k_J$, where

$$k_J \equiv \frac{a}{c_s}\sqrt{4\pi G\bar{\rho}} \tag{57}$$

is the *Jeans scale*, the combination of the last two terms leads to decaying sound waves of the form

$$\delta_{\mathbf{k}} \propto \frac{1}{\sqrt{c_s a}} \exp\left[\pm ik \int \frac{dt}{a} c_s\right]. \tag{58}$$

On large scales, or for a pressureless fluid, the last term leads to growing and decaying modes. In this regime, and changing the time variable to the scale factor a, the equation reads

$$\frac{d}{da}\left(a^3 H \frac{d\delta}{da}\right) = \frac{3}{2}\Omega_M(a)\, a\, H(a)\, \delta. \tag{59}$$

We have omitted the wavenumber label $_{\mathbf{k}}$ here, since the equation holds both in real and Fourier spaces.

Analytical solutions can be found several interesting limits:

- **Matter domination.** In this limit the equation reads

$$\frac{d^2\delta}{da^2} + \frac{3}{2a}\frac{d\delta}{da} - \frac{3}{2a^2}\delta = 0, \tag{60}$$

  which has, as growing and decaying solutions:

$$\delta(a) = \delta_+\, a + \delta_-\, a^{-3/2}. \tag{61}$$

  Overdensites thus grow proportionally to the scale factor during matter domination.

- **Λ domination.** In this limit, the equation reads

$$\frac{d^2\delta}{da^2} + \frac{3}{a}\frac{d\delta}{da} = 0, \tag{62}$$

  with solution

$$\delta(a) = \delta_+ + \delta_- a^{-3}. \tag{63}$$

- **Fluid mixture.** In the presence of non-relativistic matter and another background species with equation of state w, an analytical solution can be find of the form

$$\begin{aligned}\delta(a) =& \delta_+\, a\, {}_2F_1\left(\frac{w-1}{2w}, -\frac{1}{3w}, \frac{6w-5}{6w}; \frac{\Omega_M - 1}{\Omega_M} a^{-3w}\right) + \\ & \delta_-\, a^{-3/2}\, {}_2F_1\left(\frac{3w+2}{6w}, \frac{1}{2w}, \frac{6w+5}{6w}; \frac{\Omega_M - 1}{\Omega_M} a^{-3w}\right),\end{aligned} \tag{64}$$

  where ${}_2F_1$ is a hypergeometric function.

- **Radiation domination.** Setting $w = 1/3$ above, asymptotically we obtain, for the growing mode

$$\delta \propto \begin{cases} A + B \log a & a \ll a_{\rm eq} \\ a & a \gg a_{\rm eq}, \end{cases} \tag{65}$$

where $a_{\rm eq}$ is the scale factor at which matter and radiation contribute equally to the total energy density (the matter-radiation equality epoch).

The two main conclusions from this discussion are:

1. In the absence of pressure, and in the linear regime, overdensities grow in a **scale-independent** fashion, i.e.:

$$\delta(t, \mathbf{x}) = D(a)\, \delta(\mathbf{x}, t_*), \tag{66}$$

where $D(a)$ is the *growth factor*. The growth factor is commonly normalised such that $D(a = 1) = 1$ today (in which case $t_* = t_0$), or such that we recover the matter-dominated limit at early times: $D(a \ll 1) = a$. Unless otherwise stated, we will assume the former normalisation.

2. Growth is **linear with a during matter domination**, but stalls during either Λ domination, or during radiation domination (where the growth is at most logarithmic in a). Since the Poisson equation (Eq. 49) reads

$$\psi_k(a) = -\frac{4\pi G \bar{\rho}_0}{k^2} \frac{\delta_{\mathbf{k}}(a)}{a} \tag{67}$$

during matter domination, the gravitational potentials stay constant, and they decay in amplitude otherwise.

3 Relativistic perturbation theory

References

For more information on relativistic perturbation theory, refer to [1, 2, 3, 9, 10].

3.1 Gauge invariance

The presence of matter density inhomogeneities will result in perturbations to the background FRW metric. However, we are confronted with a problem inherent to GR. A general change of coordinates can create fictitious inhomogeneities/metric perturbations in a homogeneous Universe. Although this problem can be ignored if one expresses the final quantities of interest in terms of true observables (e.g. electromagnetic intensity measured by a particular observer), a wise choice of coordinates can often simplify otherwise lengthy calculations, or lead to equations with a simpler physical interpretation. Understanding the role of this gauge freedom is therefore important before we try to make predictions in a relativistic setting.

3.1.1 Gauge transformations for linear perturbations

Consider the case of infinitesimal changes of the form $\tilde{x}^\mu = x^\mu + \xi^\mu(x)$. How does this affect our interpretation of what a perturbation is for different types of quantities?

- **Scalars.** Consider a scalar function $\phi(x)$ which, in coordinates x^μ is composed of a "background" mode $\bar{\phi}(x)$ and a perturbation $\delta\phi$, i.e.:

$$\phi(x) = \bar{\phi}(x) + \delta\phi(x). \tag{68}$$

Since ϕ is a scalar, in the new coordinates $\tilde{\phi}(\tilde{x}) = \phi(x)$, therefore:

$$\tilde{\phi}(\tilde{x}) = \phi(x) = \phi(\tilde{x} - \xi) = \bar{\phi}(\tilde{x}) + \delta\phi(\tilde{x}) - \xi^\mu \partial_\mu \bar{\phi}, \tag{69}$$

where we have ignored all terms of higher order than 1 in $\delta\phi$ or ξ. In the new coordinates, the perturbation is therefore

$$\tilde{\delta\phi} = \delta\phi - \xi^\mu \delta_\mu \bar{\phi}. \tag{70}$$

An example of such a scalar is the energy density ρ, which can be expressed as $\rho = U^\mu U^\nu T_{\mu\nu}$.

- **Vectors.** As before, contravariant vector $V^\mu(x) = \bar{V}^\mu(x) + \delta V^\mu$. In this case, we need to take into account the transformation law for vectors, and expanding to linear order:

$$\begin{aligned}\tilde{V}^\mu(\tilde{x}) &= \frac{\partial \tilde{x}^\mu}{\partial x^\nu} V^\nu(x) \\ &= (\delta^\mu_\nu + \partial_\nu \xi^\mu)\left(\bar{V}^\nu(\tilde{x}) + \delta V^\nu - \xi^\rho \partial_\rho \bar{V}^\nu\right) \\ &= \bar{V}^\mu(\tilde{x}) + \delta v^\mu - \xi^\nu \partial_\nu \bar{V}^\mu + \bar{V}^\nu \partial_\nu \xi^\mu, \end{aligned} \tag{71}$$

  and thus the perturbation is modified as

$$\delta\tilde{V}^\mu = \delta V^\mu - \xi^\nu \partial_\nu \bar{V}^\mu + \bar{V}^\nu \partial_\nu \xi^\mu. \tag{72}$$

- **Tensors.** For a rank-2 covariant tensor, such as the metric,

$$\tilde{g}_{\mu\nu}(\tilde{x}) = \frac{\partial x^\rho}{\partial \tilde{x}^\mu}\frac{\partial x^\sigma}{\partial \tilde{x}^\nu} g_{\mu\nu}(x). \tag{73}$$

  Proceeding as in the case of vectors, we find that linear metric perturbations transform as:

$$\tilde{\delta g}_{\mu\nu} = \delta g_{\mu\nu} - \xi^\rho \partial_\rho \bar{g}_{\mu\nu} - \bar{g}_{\mu\rho}\partial_\nu \xi^\rho - \bar{g}_{\rho\nu}\partial_\mu \xi^\rho. \tag{74}$$

Inspecting Eqs. 70, 72, and 74, a general transformation law is easy to infer for tensor of arbitrary rank and index position.

3.1.2 SVT decomposition

Let us now apply the previous results to the FRW metric. The background FRW preserves the SO(3) symmetry, and therefore it makes sense to separate perturbations into the irreducible representations of this group. Under rotations, g_{00} transforms as a scalar, and therefore we can write:

$$\delta g_{00} \equiv a^2\, 2\psi. \tag{75}$$

g_{0i} is a vector. By Helmholtz's theorem, general vectors can be separated into the gradient of a scalar, and the curl of a vector (or, in other words, a component with zero divergence). Using this, we can write:

$$\delta g_{0i} = a^2(\partial_i B + S_i), \tag{76}$$

where the vector $\mathbf{S}$ must satisfy $\partial_i S_i = 0$. Finally a similar decomposition for g_{ij} yields

$$\delta g_{ij} = a^2(2\phi\eta_{ij} + 2\partial_i\partial_j E + \partial_i F_j + \partial_j F_i + h_{ij}), \tag{77}$$

where the vector $\mathbf{F}$ must also be *transverse* ($\partial_i F_i = 0$), and h is symmetric, transverse, and traceless:

$$h^i_i = 0, \quad \partial_i h^i_j = 0. \tag{78}$$

The perturbed line element therefore reads, in general:

$$d\tau^2 = a^2\left[(1+2\psi)d\eta^2 + 2(\partial_i B + S_i)d\eta\, dx^i + (-(1-2\phi)\eta_{ij} + 2\partial_i\partial_j E + \partial_i F_j + \partial_j F_i + h_{ij})dx^i\, dx^j\right].$$

Before accounting for gauge freedom, the metric perturbations are thus, in general, described by 4 scalar functions (ψ, ϕ, B, E), two transverse vector fields (F_i, S_i) (i.e. $3+3-2=4$ degrees of freedom), and a symmetric, transverse, and traceless tensor (h_{ij}) (i.e. $9-3-3-1=2$ degrees of freedom), for a total of 10 degrees of freedom.

We can similarly split the gauge perturbation ξ^μ into scalar and vector components:

$$(\xi^0, \xi^i) = (\xi^0, \partial_i\zeta + \xi^i_\perp), \tag{79}$$

where (ξ^0, ζ) are scalars, and $\xi^i_\perp$ is a transverse vector.

Applying Eq. 74 to these perturbations, we obtain the transformation laws:

$$\text{Scalars}: \quad \tilde{\psi} = \psi - a^{-1}(a\xi^0)', \quad \tilde{\phi} = \phi + \mathcal{H}\xi^0, \quad \tilde{B} = B + \zeta' - \xi^0, \quad \tilde{E} = E + \zeta. \tag{80}$$

$$\text{Vectors}: \quad \tilde{S}_i = S_i + \xi'_{\perp,i}, \quad \tilde{F}_i = F_i + \xi_{\perp,i}. \tag{81}$$

$$\text{Tensors}: \quad \tilde{h}_{ij} = h_{ij}. \tag{82}$$

Thus, scalar gauge modes only affect scalar perturbations, vectors only affect vectors, and tensor metric perturbations are gauge-invariant by construction!

Since there are two scalar gauge modes, they can be used to null out two of the scalar perturbation modes or, in other words, only two perturbation modes are gauge-invariant. Likewise, vector perturbations can be described with a single transverse vector.

If going the gauge-invariant way, the equations above can be used to construct following gauge-invariant combinations of perturbations:

$$\Psi = \psi - a^{-1}(a(B - E'))', \quad \Phi = \phi + \mathcal{H}(B - E'), \quad V_i = S_i - F_i', \quad h_{ij}. \tag{83}$$

Instead, we will pick a specific gauge, and rely on computing only pure observables (in which case the gauge we picked is irrelevant). Arguably the most commonly used gauge is the "longitudinal" or "Newtonian" gauge. This is defined by setting $B = E = 0$. Considering only scalar perturbations, the Newtonian gauge metric reads:

$$d\tau^2 = a^2 \left[(1 + 2\psi)d\eta^2 - (1 - 2\phi)|d\mathbf{x}|^2\right]. \tag{84}$$

Note that we have only included scalar modes above. In this course we will not cover vector and tensor perturbations. Fortunately, a beautiful result of cosmological perturbation theory is the fact that, at linear order, if perturbations are decomposed into their SVT components, the field equations (which we will present in the next section), for scalar, vector, and tensor modes, are actually decoupled. I.e. vector modes do not affect the evolution of scalar or tensor modes, etc. Thus, having ignored vectors and tensors will not affect the results obtained here for scalar perturbations.

3.2 Field equations for linear perturbations

3.2.1 Einstein's equations

Substituting the Newtonian gauge metric in Eq. 84 into Einsten's field equations $G_{\mu\nu} = 8\pi G\, T_{\mu\nu}$, and considering only linear terms in the metric potentials, we obtain the following set of equations:

$$\nabla^2\phi - 3\mathcal{H}(\phi' + \mathcal{H}\psi) = 4\pi G a^2\, \delta T^0_0, \tag{85}$$

$$\partial_i(\phi' + \mathcal{H}\psi) = 4\pi G a^2\, \delta T^0_i, \tag{86}$$

$$\phi'' + \mathcal{H}(2\phi + \psi)' + (2\mathcal{H}' + \mathcal{H}^2)\psi + \frac{1}{3}\nabla^2(\psi - \phi) = -\frac{4\pi}{3} G a^2\, \delta T^i_i, \tag{87}$$

$$\partial_i\partial_j(\psi - \phi) = 8\pi G a^2\, \delta T^i_j \quad (i \neq j). \tag{88}$$

The last equation is only sourced by the off-diagonal components of the perturbed energy-momentum tensor. These components are zero except for fluid species with significant shear stress. In the standard cosmological model, this is only the case for neutrinos, and the effect is very small. Thus assuming that $\phi = \psi$ is often an excellent approximation.

3.2.2 Hydrodynamical perturbations

Consider a perfect fluid, with energy-momentum tensor given by Eq. 21. The density and pressure are defined as the density and pressure measured by an observer that is co-moving with the fluid ($\rho \equiv T_{\mu\nu}U^\mu U^\nu$, $p \equiv T_{\mu\nu}(g^{\mu\nu} - U^\mu U^\nu)/3$). In the homogeneous case, $\bar{U}_\mu = (a, 0, 0, 0)$, and therefore any spatial component of U_μ denotes a small coordinate velocity of the fluid, which can be treated as a linear perturbation. In detail, we write the perturbed 4-velocity as

$$U^\mu = \left(\frac{1 - \psi}{a}, \frac{\mathbf{v}}{a}\right), \tag{89}$$

where the 0-th component is fixed by the normalisation $U^\mu U_\nu = 1$. The perturbations to the energy-momentum tensor can then be written as:

$$\delta T^0_0 = \bar{\rho}\delta, \quad \delta T^0_i = (\bar{\rho} + \bar{p})v^i, \quad \delta T^i_j = -\delta p\, \delta^i_j. \tag{90}$$

It will also be convenient to work with the *velocity divergence* $\theta \equiv \partial_i v^i$. Moreover, the spatial dependence of the equations takes a simpler form in Fourier space. For a given field $f(\mathbf{x}, \eta)$, we define its Fourier transform as

$$f(\mathbf{k}, \eta) = \int d^3\mathbf{x}\, e^{i\mathbf{k}\cdot\mathbf{x}}\, f(\mathbf{x}, \eta). \tag{91}$$

Substituting this into Einstein's equations, we obtain:

$$k^2\psi + 3\mathcal{H}(\psi' + \mathcal{H}\psi) = -4\pi G a^2\, \bar{\rho}\, \delta, \tag{92}$$

$$k^2(\psi' + \mathcal{H}\psi) = 4\pi G a^2\, (\bar{\rho} + \bar{p})\theta, \tag{93}$$

$$\psi'' + 3\mathcal{H}\psi' + (2\mathcal{H}' + \mathcal{H}^2)\psi = 4\pi G a^2\, c_s^2 \bar{\rho}\, \delta, \tag{94}$$

where, as before, $c_s^2 \equiv \delta p/\delta\rho$. Eq. 92 is the relativistic generalisation of Poisson's equation, with the second term on the right-hand side corresponding to relativistic corrections, which become relevant only on horizon-sized scales $k \lesssim \eta^{-1}$.

During matter domination ($a \propto \eta^2$, $\mathcal{H} = 2/\eta$), and assuming no pressure ($c_s^2 = 0$), Eq. 94 reads

$$\psi'' + \frac{6}{\eta}\psi' = 0, \tag{95}$$

which has solution:

$$\psi = C_1 + \frac{C_2}{\eta^5}. \tag{96}$$

Thus, as we found in the Newtonian case, during matter domination ψ does not evolve. Substituting this result into Eq. 92, discarding the decaying mode, the density perturbations then evolve as

$$\delta = \left[-\frac{(k\eta)^2}{6} - 2\right]\psi. \tag{97}$$

Hence, on sub-horizon scales, we recover the Newtonian result $\delta \propto ak^2\psi$ (as should be the case!). On superhorizon scales, relativistic effects come into play and the overdensity is frozen $\delta \simeq -2\psi$. Note, however, that the behavior on large scales is gauge-dependent, and this contribution can be completely nulled in other coordinate frames (e.g. the so-called "comoving gauge").

In a more general case, in the presence of pressure support, the behaviour can be described qualitatively in a rather generic way as

$$\psi(k, \eta) = \begin{cases} f(\eta) & k \ll 1/(c_s\eta) \\ g(\eta)e^{ic_s k\eta} & k \gg 1/(c_s\eta) \end{cases}, \tag{98}$$

where $f(\eta)$ is a slowly-varying (almost constant) function, and $g(\eta)$ is a decaying function of time. In fact, during radiation domination it's possible to find that $g \propto \eta^{-2}$ (see Problem 2).

Before we finalise this section, the following quantity is of crucial importance in cosmology:

$$\mathcal{R} \equiv -\psi - \frac{\mathcal{H}(\psi' + \mathcal{H}\psi)}{4\pi G a^2(\bar{\rho} + \bar{p})}. \tag{99}$$

This is the so-called "curvature perturbation" and has a key advantage over ψ: while we can show that ψ is constant on superhorizon scales as long as the equation of state stays constant, it undergoes small variation as the Universe transitions between different epochs (e.g. from inflation to radiation domination, and then to matter domination). In turn, it is possible to show that $\mathcal{R}$ stays constant on super-horizon scales ($k \ll aH$) **at all times** (see Problem 3).

3.2.3 Energy-momentum conservation

For a perfect fluid, the conservation of the energy-momentum tensor $\nabla_\mu T^\mu_\nu$ leads to the following two equations:

$$\nu = 0: \quad \delta' = -(1 + w)(\theta - 3\phi') - 3\mathcal{H}(c_s^2 - w)\delta, \tag{100}$$

$$\nu = i: \quad \theta' = -\mathcal{H}(1 - 3w)\theta - \frac{w'}{1 + w}\theta + \frac{c_s^2}{1 + w}k^2\delta + k^2\psi. \tag{101}$$

These equations are valid for the total $T_{\mu\nu}$ (as long as it conforms to Eq. 21), or for any individual non-interacting component. In the former case, it contains no more information than the Einstein equations (Eqs. 92-94), since the Einstein tensor automatically satisfies the Bianchi identities. In the latter case, however, the individual energy-momentum conservation equations do contain additional information, and can be used to solve for the evolution of multiple species. For interacting species, additional terms must be added to account for the momentum transfer between them. This will be the case for baryons and radiation before the decoupling epoch.

4 Inflation

References

For more information on inflation, refer to [1, 3, 4, 11].

4.1 Why inflation?

The standard "Hot Big-Bang" scenario predicts, extrapolating the evolution of a radiation-dominated Universe, an initial singularity where $a \to 0$. As we will see, this leads to a number of fundamental problems when confronted with cosmological data. The theory of inflation is arguably the most popular model to naturally solve these problems, while incidentally providing a well motivated mechanism to explain the origin of the density inhomogeneities we observe around us.

The two main problems that motivate inflation are related to the observations of the CMB:

- **The horizon problem.** The CMB is emitted at $z_d \simeq 1100$. At that point, the comoving horizon is

$$\chi_H = \int_{z_d}^{\infty} \frac{dz'}{H(z')} \simeq 250\,\text{Mpc}. \tag{102}$$

  In turn, the distance from us to the last-scattering surface is

$$\chi_{\text{LSS}} = \int_{0}^{z_d} \frac{dz'}{H(z')} \simeq 14\,\text{Gpc}. \tag{103}$$

  Thus, the horizon subtends an angle $\theta_H = \chi_H/\chi_{\text{LSS}} \sim 1^\circ$. This means that a map of the CMB should show $\mathcal{O}(10^4)$ causally-disconnected patches, and yet the temperature of the CMB is homogeneous to 1 part in 10^5 across the whole sky.

- **The curvature problem.** The curvature parameter at a given point during the Universe's evolution is

$$\Omega_k(t) = \frac{k}{(aH)^2} = \frac{k}{\dot{a}^2}. \tag{104}$$

  In a decelerating Universe, $\dot{a}$ decreases with time, and thus $|\Omega_k|$ must grow. Since CMB observations indicate that today $|\Omega_{k,0}| \lesssim 10^{-3}$, it must have been significantly smaller in the past (e.g. $|\Omega_k| \lesssim 10^{-17}$ during the nucleosynthesis epoch). Why were the initial conditions so finely tuned to give rise to a Universe that is so close to Euclidean?

The root of the horizon problem is that, if we assume a power-law expansion at early times ($a \propto t^\alpha$) the size of the horizon is finite when integrated from $t = 0$ as long as $\alpha < 1$:

$$\chi_H = \int_0^{t_d} \frac{dt}{a} \propto \frac{1}{1-\alpha}\, t^{1-\alpha}\Big|_0^{t_d} \tag{105}$$

For the integral to diverge, and thus for the size of causally-connected regions to become arbitrarily large, we need $\alpha > 1$, in which case $\ddot{a} \propto \alpha(\alpha - 1) > 0$, and the expansion must be accelerated. The horizon problem thus can only be solved through an epoch of accelerated expansion at early times.

The existence of such an epoch is also able to help with the curvature problem. Since $\Omega_k \propto \dot{a}^{-2}$, an accelerated expansion will increase $\dot{a}$, decreasing Ω_k, allowing it to take arbitrarily large values at sufficiently early times.

We will therefore define *inflation* as an epoch at early times when $\ddot{a} > 0$. Remember that this can only happen for fluids violating the strong energy condition, $p < -\rho/3$, and therefore it necessarily involves the presence of some exotic field. As we will see, the easiest and most popular way to achieve inflation usually reduces to a de Sitter-like expansion during inflation (i.e. a vacuum-dominated Universe), with

$$p = -\rho, \quad H = \text{constant}, \quad \text{and } a \propto e^{Ht}. \tag{106}$$

Before we look at specific models of inflation, let us calculate roughly how long inflation must last in order to solve the horizon problem. Let's take a toy model where inflation is exactly de-Sitter until it swiches off, with $\dot{a}/a = H_I$, and afterwards the scale factor expands as in a radiation-dominated universe ($a \propto t^{1/2}$). Let us consider three times: t_i: the start of inflation, t_e: the end of inflation, and t_0: the current time. The comoving causal horizon at the end of inflation is

$$\chi_e = \int_{t_i}^{t_e} \frac{dt}{a} = \frac{1}{a_i H_I}\left(1 - e^{-H_I(t_e - t_i)}\right) \simeq (a_i H_I)^{-1}. \tag{107}$$

Meanwhile, the comoving size of the observable Universe today is

$$\chi_o = \int_0^{t_0} dt \left(\frac{t_0}{t}\right)^{1/2} \sim H_0^{-1}. \tag{108}$$

To explain the observed homogeneity of the Universe today, we require $\chi_o < \chi_e$, which means

$$1 > \frac{a_i H_I}{H_0} = \frac{a_i}{a_e}\frac{a_e H_I}{H_0} \simeq \frac{a_i}{a_e}\left(\frac{H_I}{H_0}\right)^{1/2}, \tag{109}$$

where we have used the fact that, during radiation domination, $a \propto H^{-1/2}$.

If we identify the start of inflation with the Planck era, $H_I \sim E_{\rm Planck} \simeq 10^{19}$GeV, and use $H_0 \simeq 10^{-41}$GeV, we obtain a total number of e-folds

$$N \equiv \log(a_e/a_i) > \frac{1}{2}\log(H_I/H_0) \sim 69. \tag{110}$$

Using the GUT scale instead ($H_I \sim 10^{15}\,$GeV), the result is $N \sim 64$. Accounting for matter and Λ in the post-inflationary expansion only leads to small modifications in the prefactor of Eq. 110, and the general picture is that between 50 and 70 e-folds of inflation are needed to solve the main problems that motivate it. Finally, note that the cosmic time interval during which inflation takes place is $\Delta t = N/H_I \gtrsim 10^{-37}\,$s. So inflation is indeed very fast, assuming it takes place at these energy scales.

4.2 Scalar fields and slow roll

4.2.1 Scalar fields

Although a vacuum-dominated Universe is the simplest model for an exponentially accelerated Universe, we know that inflation must end (unlike the ongoing accelerated era!). A successful inflationary model must therefore have a *graceful exit* that allows for inflation to end, which is not possible in a pure de-Sitter Universe.

The next simplest model leading to acceleration, and allowing for a graceful exit, is a Universe dominated by a scalar field φ (which we will call the "inflaton"). In its simplest incarnation, a scalar field φ is described by a Lagrangian density

$$\mathcal{L} = \frac{1}{2} g^{\mu\nu}\nabla_\mu\varphi\nabla_\nu\varphi - V(\varphi). \tag{111}$$

In the homogeneous limit, this Lagrangian, and the associated energy-momentum tensor, are simply given by

$$\mathcal{L} = \frac{1}{2}\dot{\varphi}^2 - V(\varphi), \quad T^\mu_\nu = \text{diag}(\rho, -p, -p, -p), \tag{112}$$

with

$$\rho \equiv \frac{1}{2}\dot{\varphi}^2 + V, \quad p \equiv \frac{1}{2}\dot{\varphi}^2 - V. \tag{113}$$

The equation of motion for φ, the Klein-Gordon equation (which can also be derived from the conservation of T^μ_ν), reads:

$$\ddot{\varphi} + 3H\dot{\varphi} + V' = 0, \tag{114}$$

where we have denoted $V' \equiv dV/d\varphi$ (do not confuse this with a derivative with respect to the conformal time η). Finaly, the Friedmann equation for this fluid reads

$$H^2 = \frac{8\pi G}{3}\left[\frac{1}{2}\dot{\varphi}^2 + V\right]. \tag{115}$$

4.2.2 Slow roll

We can see from Eq. 113 that, in the regime where the field's kinetic energy is small compared to the potential, $\dot{\varphi}^2 \ll V$, φ behaves as a fluid with an effective equation of state $w = -1$, leading to an exponential expansion. Observing now, that the Klein-Gordon equation (Eq. 114) is equivalent to that of a particle in a one-dimensional potential with a friction term ($3H\dot{\varphi}$) caused by the expansion, a picture emerges that makes inflation rather natural. Consider a scalar field in a potential $V(\varphi)$ with a minimum, starting with a small velocity from a value φ_i such that $V(\varphi_i) \gg \dot{\varphi}^2$. At the start, the scalar field drives an accelerated expansion. Then, as the field rolls down the potential towards the minimum, it gathers velocity. However, the friction term slows down this descent, so that inflation can last for a long time. Eventually, the field reaches the minimum and oscillates around it, $\dot{\varphi}^2/2$ becomes larger than V, and inflation ends. This mechanism is known as "slow-roll" inflation.

For a model to be successful, during the slow-roll regime the following conditions must be satisfied:

$$\dot{\varphi}^2 \ll V, \quad \text{So as to drive an accelerated expansion.} \tag{116}$$

$$|\ddot{\varphi}| \ll 3H\dot{\varphi}, \quad \text{So that inflation lasts.} \tag{117}$$

In this approximation, Eqs. 114 and 115 simplify to a system of linear differential equations:

$$3\dot{\varphi} = -\frac{1}{H}V', \quad H^2 = \frac{8\pi G}{3}V. \tag{118}$$

It is common to define two parameters: ε, characterising whether inflation happens, and η, characterising how long it lasts:

$$\varepsilon = -\frac{\dot{H}}{H^2} = 1 - \frac{\ddot{a}a}{\dot{a}^2} \ll 1, \quad \eta = \frac{d\log\varepsilon}{d\log a} \ll 1. \tag{119}$$

For a Klein-Gordon field, these are equivalent to:

$$\varepsilon = 3\frac{\dot{\varphi}^2/2}{\dot{\varphi}^2/2 + V} \simeq \frac{M_{\rm Pl}}{2}\left(\frac{V'}{V}\right)^2, \quad \eta = 2\varepsilon - \frac{2\ddot{\varphi}}{H\dot{\varphi}} \simeq M^2_{\rm Pl}\frac{V''}{V}, \tag{120}$$

where the second approximate equality in each case holds in the slow-roll approximation. The slow-roll parameters are therefore directly related to the conditions in Eqs. 116 and 117, and can be associated with the slope and curvature of the inflaton potential.

As an example, let's study the case of a canonical quadratic potential:

$$V(\varphi) = \frac{1}{2}m^2\varphi^2. \tag{121}$$

From the Friedmann equation in the slow-roll approximation, we obtain:

$$H = q\varphi, \quad q^2 \equiv \frac{4\pi G m^2}{3}. \tag{122}$$

Subtituting this in the K-G equation:

$$\dot{\varphi} = -\frac{m^2}{3q}. \tag{123}$$

Now, for inflation to begin we need $\dot{\varphi}^2/2 \ll V$, and herefore initially the field must start at a value

$$\varphi_i \gg \frac{1}{\sqrt{12\pi G}} \sim \sqrt{2/3}M_{\rm Pl}. \tag{124}$$

We can now solve Eq. 122, then substitute in Eq. 123 to find $a(t)$. The solution is:

$$\varphi(t) = \varphi_i - \frac{m^2}{3q}t, \tag{125}$$

$$\log\left(\frac{a(t)}{a_i}\right) = 2\pi G\varphi_i^2 - \frac{m^2}{6}\left(t - \frac{3q\varphi_i^2}{m^2}\right)^2 \tag{126}$$

Now, inflation ends when Eq. 124 ceases to hold. Using Eq. 125, this happens at

$$t_e = \frac{3q\varphi_i}{m^2} - \frac{1}{m}. \tag{127}$$

Evaluating Eq. 126 at this time, we obtain the number of e-folds of inflation:

$$N = \log(a_e/a_i) = \left(\frac{\varphi_i}{2M_{\rm Pl}}\right)^2 \tag{128}$$

As expected, the field must start at high, super-Planckian values.

4.2.3 Graceful exit and reheating

As the field settles around the potential minimum, H starts decreasing, and eventually the oscillation frequency $\propto m$ becomes larger than it. In this approximation, the K-G equation reads

$$\ddot{\varphi} + m^2\varphi = 0, \quad \Rightarrow \quad \varphi \propto \cos(mt + \alpha), \tag{129}$$

where we have assumed that the minimum of the potential can be approximated as a quadratic function. In this regime, the pressure associated with the fluid is

$$p = \mathcal{L} = \frac{1}{2}(\dot{\varphi}^2 - m^2\varphi^2), \tag{130}$$

which *averages to zero over many oscillations*. Since $p = 0$, the fluid behaves, on average, as non-relativistic matter, and the Universe expands as $a \propto t^{2/3}$ (in addition to small residual oscillations). Since we do not want an empty Universe after inflation ends, the inflaton field must couple to other matter fields, to which it transfers its energy. This energy is eventually transferred into the standard model particles we know and love, through a highly speculative process that we call "reheating".

4.3 Perturbations from inflation

Soon after inflation was proposed, it was discovered that, besides solving the horizon and curvature problems, it could also provide a natural explanation for the origin of the small inhomogeneities we observe in an otherwise homogeneous Universe. Metric perturbations are sourced by quantum field fluctuations around the vacuum state that are inflated during the accelerated expansion into super-horizon scales. These re-enter the horizon after the end of inflation, and evolve into the matter density fluctuations that we observe today. Here we explore the origin and evolution of perturbations during inflation within a single-field, slow-roll framework.

Crucial to this discussion is the fact that, during inflation, the comoving hubble scale, $(aH)^{-1} = \mathcal{H}^{-1}$ decreases quickly with time (e.g. in the de-Sitter phase $\mathcal{H}^{-1} \propto \exp(-Ht)$), and conformal time $\eta \simeq -(aH)^{-1}$ takes negative values, from $-\infty$ to 0). Thus, small scales that were initially within the horizon (i.e. smaller than this scale), are quickly able to exit it. As we saw at the end of Section 3.1, curvature perturbations $\mathcal{R}$ stay constant on super-horizon scales, and are therefore a freeze-frame picture of the metric fluctuations during inflation at the time they exited the horizon. These inhomogeneities are thus pickled outside the horizon, and can survive until the end of inflation, when they re-enter the horizon and are able to evolve again. We will split our discussion in two then, studying perturbations in the inflaton field on sub-horizon scales, and then the corresponding superhorizon curvature perturbations they give rise to.

4.3.1 Sub-horizon perturbations

Consider a perturbed scalar field $\varphi(\mathbf{x},t) = \bar{\varphi}(t) + \delta\varphi(\mathbf{x},t)$. In the Newtonian gauge of a perturbed FRW metric, the Klein-Gordon equation reads[2]

$$\delta\varphi_{\mathbf{k}}'' + 2\mathcal{H}\delta\varphi_{\mathbf{k}}' + k^2\delta\varphi_{\mathbf{k}} + a^2V''\,\delta\varphi_{\mathbf{k}} - 4\bar{\varphi}'\psi_{\mathbf{k}}' + 2a^2V'\psi_{\mathbf{k}} = 0. \tag{131}$$

Since the energy-momentum tensor for a scalar field is diagonal, $\psi = \phi$. Thus, we only need one of Einstein's equation to have a complete set of ODEs. Choosing the $(0,i)$ component (Eq. 86), we obtain:

$$\psi_{\mathbf{k}}' + \mathcal{H}\psi_{\mathbf{k}} = 4\pi G\bar{\varphi}'\,\delta\varphi_{\mathbf{k}}. \tag{132}$$

In the slow-roll approximation, and on scales $k \gg |\mathcal{H}| \sim |\eta|$, the last three terms of Eq. 131 are negligible (this can be verified a posteriori). Changing variables to $f_{\mathbf{k}} \equiv a\,\delta\varphi_{\mathbf{k}}$, the equation reads:

$$f_{\mathbf{k}}'' + \left(k^2 - \frac{a''}{a}\right) f_{\mathbf{k}} = 0. \tag{133}$$

On small scales, the second term in parentheses can be ignored, and the field evolves as a harmonic oscillator

$$\delta\varphi_{\mathbf{k}} = C_{\mathbf{k}}\frac{e^{\pm ik\eta}}{a}. \tag{134}$$

Now, can we think of a physical criterion to fix the initial condition amplitude $C_{\mathbf{k}}$?

4.3.2 Quantization and vacuum fluctuations

A field cannot be perfectly homogeneous, as soon as quantum effects are taken into account. Even if we assume that the system is in its lowest possible energy state (the *vacuum*), there is an inherent uncertainty to what its true value is at all points in space. We can therefore determine the amplitude of $\delta\varphi_{\mathbf{k}}$ by considering the minimum fluctuation amplitude allowed by QFT. To do so, we first need to quantise the field.

This is straightforward to do for a canonical scalar field such as f. We promote $f_{\mathbf{k}}$ to an operator $\hat{f}_{\mathbf{k}}$ and, for convenience, write it in terms of ladder operators $\hat{a}_{\mathbf{k}}$ and $\hat{a}_{\mathbf{k}}^\dagger$:

$$\hat{f}_{\mathbf{k}}(\eta) = f_k(\eta)\hat{a}_{\mathbf{k}} + f_k^*(\eta)\hat{a}_{\mathbf{k}}^\dagger, \tag{135}$$

where f_k is the positive-energy solution to the K-G equation

$$f_k(\eta) = \frac{e^{-ik\eta}}{\sqrt{2k}}, \tag{136}$$

the ladder operators satisfy the commutation relation

$$[\hat{a}_{\mathbf{k}}, \hat{a}_{\mathbf{k}'}^\dagger] = (2\pi)^3\delta^D(\mathbf{k}-\mathbf{k}'), \tag{137}$$

and the vacuum state $|0\rangle$ satisfies $\hat{a}_{\mathbf{k}}|0\rangle = 0$. As a reminder: the specific normalisation and choice of frequency of $f_k(\eta)$ guarantees that $\hat{f}$ satisfies the appropriate commutation relation with its conjugate momentum field, and that the vacuum $|0\rangle$ is the minimum-energy state of the Hamiltonian.

The vacuum expectation value (VEV) of the field is therefore $\langle\hat{f}_{\mathbf{k}}\rangle \equiv \langle 0|\hat{f}|0\rangle = 0$, while its variance is:

$$\langle\hat{f}_{\mathbf{k}}^\dagger\hat{f}_{\mathbf{k}'}\rangle = \langle 0|\hat{f}_{\mathbf{k}}^\dagger\hat{f}_{\mathbf{k}'}|0\rangle = P_f(k,\eta)(2\pi)^3\delta^D(\mathbf{k}-\mathbf{k}'). \tag{138}$$

This defines the power spectrum of any field $\hat{f}$. In our case, this is given by

$$P_f(k,\eta) = |f_k(\eta)|^2 = \frac{1}{2k}. \tag{139}$$

The picture that arises is thus the following: inhomogeneities are sourced by quantum fluctuations in the inflaton field on sub-horizon scales. The inhomogeneities we observe are therefore one realisation of those allowed by the quantum theory. The theory does not determine the values of the particular

[2] Remember that, confusingly, $\delta\varphi' \equiv \partial_\eta\delta\varphi$, but $V' \equiv dV/d\varphi$.

realisation, but it does provide predictions for its statistical cumulants (e.g. the power spectrum). Effectively, this allows us to treat the perturbation variable $\hat{f}_{\mathbf{k}}$ as a stochastic field of the form

$$f_{\mathbf{k}}(\eta) = a_{\mathbf{k}} \frac{e^{-ik\eta}}{\sqrt{2k}}, \tag{140}$$

where the random field $a_{\mathbf{k}}$ satisfies the statistics

$$\langle a_{\mathbf{k}} \rangle = 0, \quad \langle a^*_{\mathbf{k}} a_{\mathbf{k}'} \rangle = (2\pi)^3 \delta^D(\mathbf{k} - \mathbf{k}'). \tag{141}$$

This will come in very handy in what follows!

To summarize, the sub-horizon perturbation to the inflaton takes the form:

$$\delta\varphi_{\mathbf{k}} = a_{\mathbf{k}} \frac{e^{-ik\eta}}{a\sqrt{2k}}, \tag{142}$$

where $a_{\mathbf{k}}$ is a random field with a unit power spectrum.

4.3.3 The primordial scalar spectrum

As a given perturbation exits the horizon during inflation (i.e. when $k < aH$), the term proportional to k^2 in Eq. 131 becomes subdominant, and the oscillatory behaviour ceases (as we are now used to). Tracking perturbations outside the horizon, especially during a transition in the background expansion, such as the end of inflation, is easiest in terms of the curvature perturbation $\mathcal{R}$. Using Eq. 99, and assuming slow roll, the relation between $\mathcal{R}$ and $\delta\varphi$ becomes

$$\mathcal{R}_{\mathbf{k}} = -\frac{H}{\dot{\bar{\varphi}}} \delta\varphi_{\mathbf{k}} \tag{143}$$

Let us define the dimensionless primordial power spectrum $\Delta^2_{\mathcal{R}}(k)$ as the variance of $\mathcal{R}_{\mathbf{k}}$ at the time of horizon exit (after which, $\mathcal{R}$ is constant) as:

$$\langle \mathcal{R}^*_{\mathbf{k}} \mathcal{R}_{\mathbf{k}'} \rangle \equiv \frac{2\pi^2}{k^3} \Delta^2_{\mathcal{R}}(k)\, (2\pi)^3 \delta^D(\mathbf{k} - \mathbf{k}'). \tag{144}$$

I.e. the relation between $\Delta^2_{\mathcal{R}}$ and $P_{\mathcal{R}}$ is

$$\Delta^2_{\mathcal{R}}(k) = \frac{k^3}{2\pi^2} P_{\mathcal{R}}(k). \tag{145}$$

The dimensionless power spectrum is often preferred to $P_{\mathcal{R}}$ because it is dimensionless (as its name suggests), and represents the amount of variance in the field per logarithmic interval of wavenumber k.

Combining Eqs. 142 and 143, we find

$$\Delta^2_{\mathcal{R}}(k) = \frac{k^3}{2\pi^2} \frac{H^2}{\dot{\bar{\varphi}}^2} \frac{1}{2ka^2}\bigg|_{k=aH} = \frac{1}{2M^2_{\rm Pl}\varepsilon} \left(\frac{H}{2\pi}\right)^2 \bigg|_{k=aH}, \tag{146}$$

where ε is the slow-roll parameter of Eq. 120. During slow roll, both H and ε are almost constant, and thus we arrive at one of the key predictions of inflation: an *almost-scale-invariant primordial power spectrum*. The small time variation in ε and H towards the end of inflation will endow $\Delta_{\mathcal{R}}$ with some scale dependence. This is usually parametrised in terms of a spectral index n_s, defined as

$$n_s - 1 \equiv \frac{d\log \Delta^2_{\mathcal{R}}}{d\log k}. \tag{147}$$

From Eq. 146, this can be written in terms of the slow-roll parameters

$$n_s - 1 = -2\varepsilon - \eta, \tag{148}$$

and thus departures from $n_s = 1$ must be small.

x_e	$z_{\rm Saha}$	$z_{\rm exact}$
0.5	1370	1210
0.1	1250	980
0.01	1140	820

Table 1: Estimates of the recombination redshift using Saha's equation and the exact non-equilibrium result.

5 The Cosmic Microwave Background

The Cosmic Microwave Background (CMB) is the observable that has allowed cosmologists to make the most precise measurements of the abundances of the main energy species, the current expansion rate, and the spectrum of primordial perturbations. The CMB has its origin in the *epoch of recombination*. As the Universe expanded, and the background radiation cooled down, electrons and protons were able to form neutral hydrogen atoms before being immediately reionised. As the density of free electrons sharply decreased, the photons effectively ceased to interact with them via Thomson scattering, and were able to travel freely. The resulting background of photons (the CMB) has an almost perfect black-body spectrum, and spatial fluctuations in the temperature of this spectrum provide us with a picture of the cosmic perturbations at the time of recombination. Here we will try to provide a brief description of these fluctuations using the tools from perturbation theory we developed in Section 3, connecting them with the primordial metric perturbations predicted by inflation, and discussed in Section 4.

References

For more information on the physics of the CMB, refer to [1, 3, 2, 9, 10].

5.1 Recombination

When did recombination happen? A quick, but highly inaccurate calculation would tell us that, since the ionization potential of the neutral hydrogen atom in its fundamental state is $\chi = 13.6\,\text{eV}$, and the CMB temperature today is $T_{\rm CMB} = 2.7255\,\text{K}$, recombination must have happened at redshift

$$1 + z_{\rm rec} = \frac{\chi}{k_B T_{\rm CMB}} \sim 5 \times 10^4, \tag{149}$$

deep in the radiation-dominated era. **This is a wild over-estimation!**

A better (but still inaccurate) estimate, can be made by assuming that, while recombination takes place, the neutral and ionised hydrogen, as well as the free electrons, are in thermal equilibrium. This will be good enough as long as the recombination rate is much higher than the expansion rate. In this case, the densities of the three species are related by the *Saha equation*:

$$\frac{n_{\rm HII} n_e}{n_{\rm HI}} = \left(\frac{2\pi m_e k_B T}{h_P^2}\right)^{3/2} e^{-\chi/k_B T}. \tag{150}$$

This can be rewritten in terms of the ionisation fraction $x_e \equiv n_e/(n_{\rm HI} + n_{\rm HII})$, and the baryon density parameter $\omega_b \equiv \Omega_b h^2$ as

$$\frac{x_e^2}{1 - x_e} = \frac{5.8 \times 10^{15}}{\omega_b T_4^{3/2}} e^{-15.8/T_4}, \tag{151}$$

where $T_4 \equiv T/(10^4\,\text{K})$. Solving for T_4 as a function of x_e (which must be done numerically), and remembering that $1 + z = T/T_{\rm CMB}$, we obtain the estimates in the second column of Table 1.

According to this calculation, by redshift $z \sim 1250$, well in the matter-dominated regime, the Universe is $\sim 90\%$ neutral. The huge difference with respect to the naive calculation is due to the low baryon density in our Universe, which means that the photons in the tail of the blackbody spectrum are able to keep the Universe ionised even when the blackbody peak has redshifted significantly below the ionisation energy.

The equilibrium calculation gets qualitatively the right answer: recombination happens during matter domination, at around $z \sim 1000$. A full non-equilibrium calculation, accounting for the recombination rates to different excited states, and the transitions between them, obtains the results in the third column of Table 1. As it turns out, the equilibrium approximation is not a very good one! This is because the non-thermal photons created when an atom recombines directly to the ground state, or those due to the Lyman-α transition, enhance the blackbody tail. Recombination must take place through forbidden channels (e.g. the $2s \to 1s$ transition), making the effective recombination rate comparable with the expansion rate, spoiling the equilibrium assumption.

5.2 Perturbations before and after recombination

5.2.1 The perturbation equations

At the time of recombination, the following set of 7 perturbation play a central role in setting the properties of the CMB temperature fluctuations:

- δ_c and θ_c: the overdensity and velocity divergence of the cold dark matter.
- δ_b and θ_b: the overdensity and velocity divergence of baryonic matter.
- δ_γ and θ_γ: the overdensity and velocity divergence of radiation.
- ψ: the metric potential.

The cold dark matter is de-coupled from the other species, and thus follows its own conservation laws (Eqs. 100 and 101):

$$\delta_c' + \theta_c - 3\phi' = 0, \quad \theta_c' + \mathcal{H}\theta_c - k^2\psi = 0. \tag{152}$$

The photons and baryons are tightly coupled before recombination, and thus their conservation laws must include the transfer of momentum between both species via Thomson scattering. The result is

$$\delta_b' + \theta_b - 3\phi' = 0, \quad \theta_b' + \mathcal{H}\theta_b - k^2\psi = c_{s,b}^2 k^2 \delta_b + \frac{4\bar{\rho}_\gamma}{3\bar{\rho}_b} a\, n_e\, \sigma_T (\theta_\gamma - \theta_b) \tag{153}$$

$$\delta_\gamma' + \frac{4}{3}\theta_\gamma - 4\phi' = 0 \quad \theta_\gamma' - k^2\psi = \frac{1}{4}k^2\delta_\gamma + a\, n_e\, \sigma_T (\theta_b - \theta_\gamma), \tag{154}$$

where σ_T is the Thomson scattering cross-section, and $c_{s,b}^2$ is the sound speed in the baryon fluid. Finally, we need one more equation for ψ. For this, we can use any of the three independent Einstein's equations (Eqs. 92-94), for instance, the relativistic Poisson's equation

$$k^2\psi + 3\mathcal{H}(\psi' + \mathcal{H}\psi) = -4\pi G a^2\, \bar{\rho}\, \delta, \tag{155}$$

where $\bar{\rho} = \bar{\rho}_c + \bar{\rho}_b + \bar{\rho}_\gamma$, and

$$\delta = \frac{\bar{\rho}_c}{\bar{\rho}}\delta_c + \frac{\bar{\rho}_b}{\bar{\rho}}\delta_b + \frac{\bar{\rho}_\gamma}{\bar{\rho}}\delta_\gamma. \tag{156}$$

The evolution of the cold dark matter component is simple: since recombination takes place during matter domination, CDM dominates over the baryons and radiation, and sets the gravitational potentials via Poisson's equation (i.e. $\delta \sim \delta_c$). δ_c thus evolves as we discussed in Section 2, as $\delta_c \propto a$.

Calculating the evolution of the baryon-photon fluid is more complicated, due to the transfer of momentum between them. The behaviour can be understood, however, by using the "tight-coupling approximation": before recombination baryons and photons are tightly coupled, and the baryon-photon fluid can be thought of as a single coupled fluid with an effective sound speed and some viscosity (caused by Thomson scattering). The origin of this sound speed is easy to understand: the photons drag the baryons via Thomson scattering, and thus the baryons feel the radiation pressure. Thus, pressure waves develop in the baryon-photon fluid (as we saw when solving Jeans' equation). On scales below the photon mean free path, viscosity due to Thomson scattering damps the amplitude of these waves exponentially. After recombination, photons and baryons decouple. The baryons follow the pressureless Jeans' equation (like the CDM), falling into the gravitational potentials set by the dark matter, and contributing to them. Shortly afterwards, CDM and baryons mix into a single non-relativistic fluid with the same evolution and scale dependence.

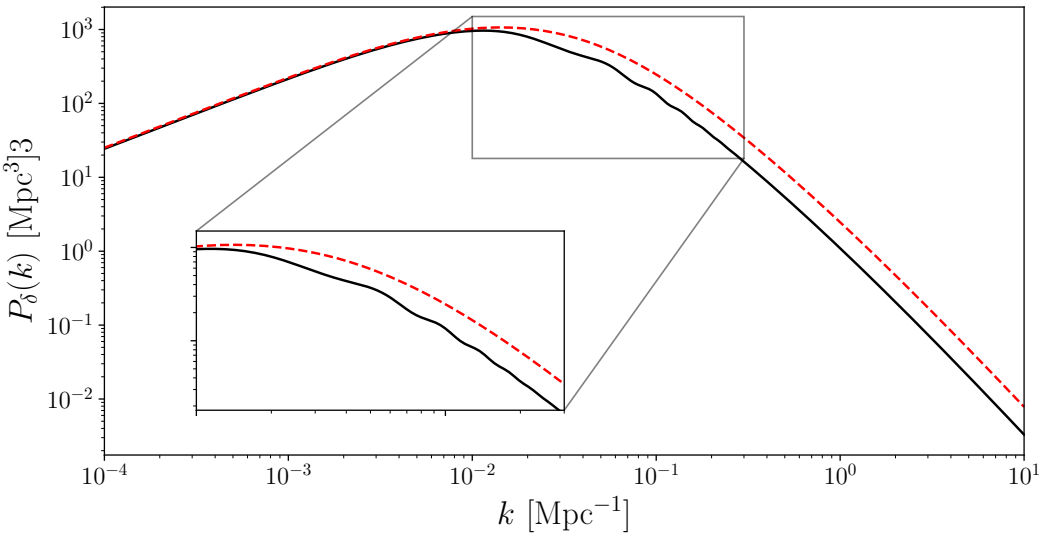

Figure 1: Linear matter power spectrum without (dashed red) and with (solid black) a baryonic component.

5.2.2 The linear matter power spectrum

Although this is not directly related to the CMB itself, the discussion in the previous section provides us with all the tools to understand the shape of a key ingredient in the evolution of cosmic structures: the linear matter power spectrum after recombination. We are therefore not able to resist the temptation to discuss that here!

On sub-horizon scales, we can make use of the non-relativistic Poisson's equation to relate the matter fluctuations and the gravitational potential (Eq. 49):

$$\delta_k = -\frac{a\,k^2}{Q}\psi_k, \quad Q \equiv 4\pi G\bar{\rho}_0 = \frac{3}{2}H_0^2\Omega_{M,0}. \tag{157}$$

On these same scales, we can approximate $\psi \sim \mathcal{R}$. Perturbations re-entering the horizon after inflation will do so either during radiation domination or during matter domination. Perturbations on the largest scales will re-enter later, during the matter-domination era. Since ψ does not evolve during matter domination, these perturbations thus preserve their amplitude. On smaller scales, perturbations enter the horizon during radiation domination and therefore their amplitude decreases approximately as $1/\eta^2$ (see Eq. 98). Smaller modes have a stronger suppression, since they entered the horizon earlier. Since re-entry happens when $k \sim \eta$, the suppression factor is $\propto k^{-2}$. After matter-radiation equality $\eta_{\rm eq}$, these modes preserve their amplitude. Therefore, during matter domination, the scale dependence of the gravitational potential is, approximately:

$$\frac{\psi(k,\eta)}{\mathcal{R}(k,\eta_*)} = \begin{cases} 1 & k \ll k_{\rm eq} \\ \left(\frac{k_{\rm eq}}{k}\right)^2 & k \gg k_{\rm eq} \end{cases}, \tag{158}$$

where η_* is some early time before any of these modes re-entered the horizon, and we have defined the equality scale $k_{\rm eq} \equiv \eta_{\rm eq}^{-1}$.

During matter domination, the matter power spectrum is thus related to the primordial power spectrum via:

$$P_\delta(k) \propto k^4 P_\psi(k) \propto k^4 \left(\frac{\psi(k,\eta)}{\mathcal{R}(k,\eta_*)}\right)^2 P_{\mathcal{R}}(k) \propto k \left(\frac{\psi(k,\eta)}{\mathcal{R}(k,\eta_*)}\right)^2 \Delta^2_{\mathcal{R}}(k). \tag{159}$$

Then, using $\Delta^2_{\mathcal{R}} \propto k^{n_s-1}$:

$$P_\delta(k) \propto \begin{cases} k^{n_s} & k \ll k_{\rm eq} \\ k^{n_s-4} & k \gg k_{\rm eq} \end{cases}. \tag{160}$$

With $n_s \sim 1$ we therefore expect a kink at $k = k_{\rm eq}$. This is shown as the dashed red lines in Fig. 1.

Including the impact of the baryonic component in the linear matter power spectrum involves two effects:

- First, a slight decrease in amplitude on smaller scales, since the overdensity in the baryonic component was not able to grow effectively before recombination.
- Second, an oscillatory component caused by the acoustic oscillations in the baryon-photon fluid before recombination (these are the so-called "baryon acoustic oscillations", BAOs). Their amplitude is significantly smaller than the oscillations we'll see in the CMB power spectrum, although they reproduce the same small-scale damping. Their comoving frequency is the so-called sound horizon:

$$r_s \equiv \int^{\eta_d} d\eta \, c_s. \tag{161}$$

The resulting power spectrum is shown black in Fig. 1.

The evolution of this spectrum in time, during matter or Λ domination is simply through a multiplicative time-dependent factor since, as we saw, growth is self-similar in this regime (see Eq. 66). The growth factor is $D(z) \propto a = 1/(1+z)$ during matter domination, and then decelerates after entering the Dark Energy era. It is hoped, that studying the evolution in structure growth may thus shed light onto the nature of Dark Energy, and potentially provide evidence for deviations from a perfect cosmological constant.

OK, back to the main topic of this section: the CMB.

5.3 Temperature anisotropies and the CMB power spectrum

The CMB anisotropies are fluctuations in the temperature of photons emitted during recombination, and observed today. Since the temperature determines the properties of the black-body spectrum, a rigorous derivation of all the terms contributing to the observed temperature fluctuation requires solving for the evolution of the photon distribution function, by solving the Boltzmann equation, including the contribution from Thomson scattering before and during recombination. We can, however, get a reasonably good description of the temperature fluctuations by making two approximations:

- We will assume "instantaneous recombination". The CMB photons were emitted exactly at the time recombination happened. We can define this as whenever the ionization fraction reached a particular threshold. The results are not too sensitive to this, since recombination is indeed quite fast.
- Instead of solving the Boltzmann equation, we will quantify how the frequency of a single photon changes as it propagates. Since the peak of the blackbody spectrum is at $\nu \propto k_B T/h$, we can estimate the temperature fluctuation as

$$\frac{\delta T}{\bar{T}} = \frac{\delta \nu}{\bar{\nu}}, \tag{162}$$

  where barred quantities are those in an unperturbed Universe, and $\nu = \bar{\nu} + \delta\nu$.

We will therefore start by studying the propagation of photons in a perturbed FRW metric, before examining the different contributions to the CMB power spectrum.

5.3.1 Photon propagation in a perturbed Universe

Photons move along null geodesics, and therefore the photon 4-momentum $p^\mu \equiv dx^\mu/d\lambda$ satisfies:

$$\dot{p}^\mu + \Gamma^\mu_{\nu\sigma} p^\mu p^\sigma = 0, \quad p^\mu p^\nu g_{\mu\nu} = 0, \tag{163}$$

where here $\dot{p}$ denotes derivatives with respect to an affine parameter λ (we will use η as a time variable here). In the Newtonian gauge, these read:

$$\dot{p}^0 + \left[\mathcal{H} + 2\frac{d\psi}{d\eta} - \psi'\right](p^0)^2 + [\mathcal{H}(1-2\phi-2\psi) - \phi']|\mathbf{p}|^2 = 0, \tag{164}$$

$$\dot{p}^i + \left[2\mathcal{H} - 2\frac{d\phi}{d\eta}\right] p^i p^0 + \partial_i\psi(p^0)^2 + \partial_i\phi|\mathbf{p}|^2 = 0, \tag{165}$$

$$(p^0)^2(1+2\psi) - |\mathbf{p}|^2(1-2\phi) = 0. \tag{166}$$

Here $d/d\eta$ indicates total derivatives with respect to η along the photon trajectory:

$$\frac{d\alpha}{d\eta} \equiv \alpha' + \frac{p^i}{p^0}\partial_i\alpha, \quad \alpha' \equiv \partial_\eta\alpha. \tag{167}$$

Consider now a comoving observer (i.e. an observer with $dx^i = 0$), with 4-velocity $u_c^\mu = a^{-1}(1-\psi)\delta_0^\mu$. The equations above can be simplified by changing variables to the comoving energy $\epsilon \equiv a p_\mu u_c^\mu$, and the direction vector $\hat{\mathbf{e}} \equiv \mathbf{p}/|\mathbf{p}|^2$. These are related to the components of the 4-momentum via:

$$\frac{d\eta}{d\lambda} \equiv p^0 = a^{-2}\epsilon(1-\psi), \quad \frac{d\mathbf{x}}{d\eta} \equiv \frac{\mathbf{p}}{p^0} = (1+\psi+\phi)\hat{\mathbf{e}}. \tag{168}$$

Since ϵ and $\hat{\mathbf{e}}$ are constant in an unperturbed FRW metric, the geodesic equations in terms of these variables are directly sourced by first-order terms. These are:

$$\frac{1}{\epsilon}\frac{d\epsilon}{d\eta} = -\frac{d\psi}{d\eta} + \psi' + \phi', \tag{169}$$

$$\frac{d\hat{\mathbf{e}}}{d\eta} = -\nabla_\perp(\phi+\psi), \tag{170}$$

where we have defined the transverse gradient $\nabla_\perp \equiv \nabla - \hat{\mathbf{e}}(\hat{\mathbf{e}}\cdot\nabla)$.

These equations can be readily integrated along the unperturbed photon trajectory (which is correct to first order in the perturbations), obtaining,

$$\frac{\epsilon}{\epsilon_0} = 1 + \psi_0 - \psi + \int_{\eta_0}^{\eta} d\eta'\,(\phi' + \psi') \tag{171}$$

$$\mathbf{x}(\eta) = -\hat{\mathbf{e}}_0\int_\eta^{\eta_0} d\eta'\,(1+\phi+\psi) - \int_\eta^{\eta_0} d\eta'(\eta'-\eta)\nabla_\perp(\phi+\psi). \tag{172}$$

where the subscript $_0$ denotes quantities evaluated at Earth.

The photon frequency measured by an observer with 4-velocity u^μ is $h_P\nu = p^\mu u_\mu$. An observer with peculiar velocity $\mathbf{v}$ has a 4-velocity $u^\mu = a^{-1}(1-\psi, \mathbf{v})$, and therefore the frequency can be related to the variable ϵ via:

$$h_P\nu = a^{-1}\epsilon(1 + \hat{\mathbf{n}}\cdot\mathbf{v}), \tag{173}$$

where $\hat{\mathbf{n}}$ is the line-of-sight unit vector $\hat{\mathbf{n}} = -\hat{\mathbf{e}}$. The observed and emitted frequencies are therefore related via the perturbed redshift relation:

$$\frac{\nu}{\nu_0} = 1 + z = \frac{1}{a}\left[1 - \psi + \psi_0 + \hat{\mathbf{n}}\cdot(\mathbf{v} - \mathbf{v}_0) + \int_{\eta_0}^{\eta} d\eta'\,(\phi' + \psi')\right] \tag{174}$$

The three perturbation terms on the right hand side of this equation have clear physical interpretations:

- $\psi_0 - \psi$ represents the effect of gravitational redshifting as photons climb out of the potential at the source and fall into that at the observer. This is often called the "Sachs-Wolfe" effect.
- $\hat{\mathbf{n}}\cdot(\mathbf{v} - \mathbf{v}_0)$ is the standard Doppler redshifting.
- $\int d\eta\,(\phi' + \psi')$ is the so-called "Integrated Sachs-Wolfe" effect (ISW for short). Photons will get a net energy loss or gain (redshift or blueshift) if the potential wells evolve while they are being traversed. As we saw, the gravitational potential only evolves during radiation and Λ domination, giving rise to the "early" and "late" ISW effects.

Using Eq. 162, the observed temperature fluctuation is related to the temperature fluctuation at recombination via:

$$\left.\frac{\delta T}{T}\right|_0 = \left(\frac{\delta T}{T} + \psi - \hat{\mathbf{n}}\cdot\mathbf{v}\right)_{\rm rec} + \int_{\eta_{\rm rec}}^{\eta_0} d\eta(\phi' + \psi'). \tag{175}$$

Note that we have discarded the terms dependent on the gravitational potential and the peculiar velocity at the observer, since they only contribute to the monopole ($\ell = 0$) and dipole ($\ell = 1$) of the temperature fluctuations. Finally, using the Stefan-Boltzmann law $\rho_\gamma \propto T^4$, the temperature fluctuation at recombination can be related to the radiation overdensity as $\delta T/T = \delta_\gamma/4$, and we obtain the final result:

$$\frac{\delta T}{T}(\hat{\mathbf{n}}) = \left(\frac{\delta_\gamma}{4} + \psi - \hat{\mathbf{n}}\cdot\mathbf{v}\right)(\eta_{\rm rec}, \chi_{\rm rec}\hat{\mathbf{n}}) + \int_{\eta_{\rm rec}}^{\eta_0} d\eta\,(\phi' + \psi')(\eta, \chi\hat{\mathbf{n}}), \tag{176}$$

where the comoving distance along the unperturbed photon trajectory is $\chi = \eta_0 - \eta$.

5.3.2 Angular power spectra

The temperature fluctuation $\delta T/T$ is a quantity defined on the sphere. The natural basis to decompose such a quantity is the spherical harmonics:

$$\frac{\delta T}{T}(\hat{\mathbf{n}}) = \sum_{\ell m} a_{\ell m}\, Y_{\ell m}(\hat{\mathbf{n}}), \qquad a_{\ell m} = \int d\hat{\mathbf{n}}\, \frac{\delta T}{T}(\hat{\mathbf{n}})\, Y^*_{\ell m}(\hat{\mathbf{n}}). \tag{177}$$

For a statistically isotropic field, such as $\delta T/T$, the angular power spectrum C_ℓ is defined in analogy to the power spectrum $P(k)$ as:

$$\langle a_{\ell m} a^*_{\ell' m'}\rangle = C_\ell\, \delta_{\ell\ell'}\delta_{mm'}. \tag{178}$$

Our goal now is to connect the angular power spectrum of the CMB with the primordial power spectrum $\Delta^2_{\mathcal{R}}(k)$.

Consider a quantity $f(\hat{\mathbf{n}})$, defined on the sphere in terms of a radial lightcone integral over a three-dimensional quantity $F(\mathbf{x}, \eta)$:

$$f(\hat{\mathbf{n}}) = \int^{\eta_0} d\eta\, q_f(\chi) F(\chi\hat{\mathbf{n}}, \eta), \tag{179}$$

where $q_f(\chi)$ is a radial kernel. Assume now that the three-dimensional quantity is linearly related to the primordial curvature perturbation $\mathcal{R}_{\mathbf{k}}$ through a transfer function $T_F(k, \eta)$, such that

$$F_{\mathbf{k}}(\eta) = T_F(k, \eta)\, \mathcal{R}_{\mathbf{k}}. \tag{180}$$

The harmonic coefficients of f are then related to $\mathcal{R}_{\mathbf{k}}$ through:

$$f_{\ell m} = \int \frac{dk}{2\pi^2} k^2\, \Delta^f_\ell(k) i^\ell \int d\hat{\mathbf{n}}_{\mathbf{k}}\, Y^*_{\ell m}(\hat{\mathbf{n}}_{\mathbf{k}})\, \mathcal{R}_{\mathbf{k}}, \tag{181}$$

where $\hat{\mathbf{n}}_{\mathbf{k}} \equiv \mathbf{k}/k$, and

$$\Delta^f_\ell(k) = \int d\chi\, q_v(\chi)\, T_F(k, \eta)\, j_\ell(k\chi). \tag{182}$$

This can be proven by separating F into its Fourier coefficients, and using the plane-wave expansion:

$$e^{i\mathbf{k}\cdot\mathbf{x}} = 4\pi \sum_{\ell m} i^\ell\, j_\ell(k\chi)\, Y_{\ell m}(\hat{\mathbf{n}})\, Y^*_{\ell m}(\hat{\mathbf{n}}_{\mathbf{k}}), \tag{183}$$

where $j_\ell(x)$ is the spherical Bessel function of order ℓ.

The angular power spectrum of f can then be found by squaring $f_{\ell m}$ and taking the ensemble average over realisations of the primordial metric fluctuations. Using Eq. 144, the result is:

$$C^f_\ell = \frac{2}{\pi}\int \frac{dk}{k}\, |\Delta^f_\ell(k)|^2\, \Delta^2_{\mathcal{R}}(k). \tag{184}$$

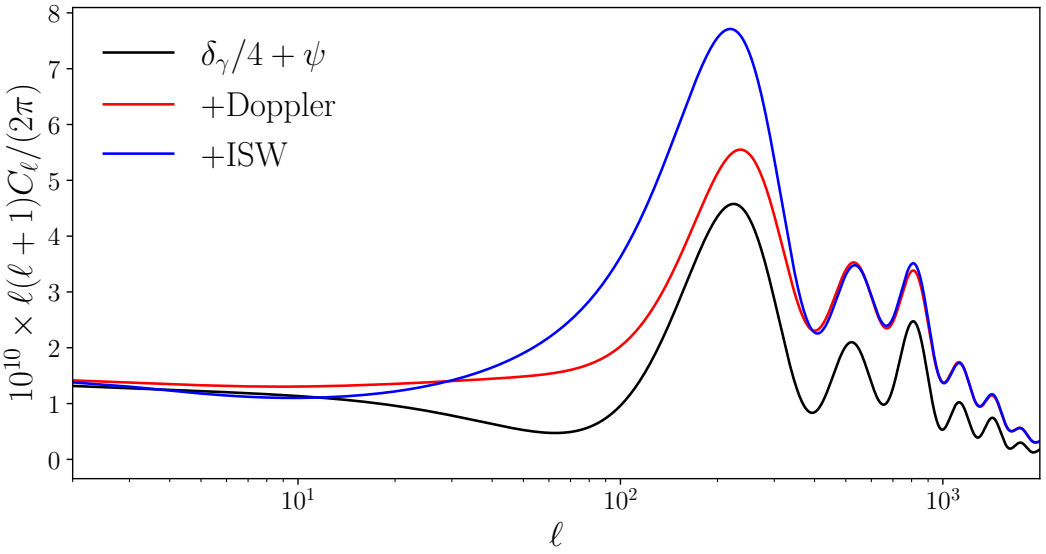

Figure 2: Angular power spectrum of the CMB temperature fluctuations. The black line shows the contribution from the density and Sachs-Wolfe terms. The red and blue lines then show the result of including the Doppler and ISW terms (in this order).

In general, a projected quantity, such as the CMB temperature fluctuation, may be a sum of several contributions: $f(\hat{\mathbf{n}}) = \sum_\alpha f_\beta(\hat{\mathbf{n}})$. In this case the previous expression generalises trivially to

$$C_\ell^f = \frac{2}{\pi}\int \frac{dk}{k}\left(\sum_{\alpha\beta}\Delta_\ell^\alpha(k)\Delta_\ell^\beta(k)\right)\Delta^2_{\mathcal{R}}(k). \tag{185}$$

Note that, while this treatment applies to the δ_γ, Sachs-Wolfe and ISW terms in Eq. 176, we must modify the definition of Δ_ℓ^f for Doppler-like terms of the form

$$g(\hat{\mathbf{n}}) = \int^{\eta_o} d\eta\, q_g(\chi)\,\hat{\mathbf{n}}\cdot\mathbf{v}. \tag{186}$$

It is easy to show that, in this case, the angular transfer function reads:

$$\Delta_\ell^g(k) = -\int d\chi\, q_g(\chi)\,\chi\, T_\theta(k,\eta)\frac{j'_\ell(k\chi)}{k\chi}, \tag{187}$$

where T_θ is the transfer function for the velocity divergence, and $j'_\ell(x) \equiv dj_\ell(x)/dx$.

Figure 2 shows the angular power spectrum of the CMB temperature fluctuations, separated into its different contributions. Although the density term is responsible for setting the structure of acoustic peaks, associated with the pressure waves in the baryon-photon fluid, the Doppler and ISW contributions are not subdominant, and must always be taken into account in the calculation. It is worth noting that the ISW term is dominated by the early ISW contribution, whereas the late-time contribution, due to Dark Energy, is negligible in the CMB power spectrum. The late ISW effect has been detected, however, by cross-correlating CMB maps with probes of the late-time structure such as galaxies, which trace the time-varying potentials that give rise to this effect. This measurement can be used to put constraints on the Dark Energy abundance.

6 Gravitational lensing

At late times, most cosmological information from metric perturbations comes from the study of the inhomogeneities in the matter density. Although nature has provided us with a wide variety of *proxies* for these inhomogeneities, such as the distribution of galaxies, or the fluctuations in gas pressure and

density from observations of the Sunyaev Zel'dovich effect and the Lyman-α forest, the only *direct* observations of the matter overdensities are those based on gravitational lensing. Here we provide a very quick review of the theory of "weak lensing", the regime in which gravitational lensing causes only small variations in the photon path, and how it are utilised in modern cosmology.

References

For more information on weak gravitational lensing for cosmology, refer to [2, 12, 13].

6.1 Lensing potential, deflection, convergence and shear

As we derived in Section 5.3.1, metric perturbations modify photon trajectories and energies, and thus cause observers to assign angular coordinates that differ from those of the point from which the photon originated. Keeping only the transverse part of Eq. 172, and changing the time variable from η to the radial coordinate along the unperturbed geodesic $\chi = \eta_0 - \eta$, the equation reads:

$$\delta\vec{\boldsymbol{\theta}} = \int_0^{\chi_s} d\chi \left(1 - \frac{\chi}{\chi_s}\right) \nabla_\perp(\phi + \psi), \tag{188}$$

where χ_s is the radial coordinate of the source, and $\delta\vec{\boldsymbol{\theta}} \equiv \mathsf{P}^\perp_{\hat{\mathbf{n}}}(\hat{\mathbf{n}} - \hat{\mathbf{n}}_s)$ is the difference between the observed arrival direction ($\hat{\mathbf{n}}$) and the true angular coordinates of the source $\hat{\mathbf{n}}_s \equiv \mathbf{x}/\chi_s$. Here, $\mathsf{P}^\perp_{\hat{\mathbf{n}}} \equiv \mathbb{1} - \hat{\mathbf{n}}\hat{\mathbf{n}}^T$ is the projector onto the space perpendicular to the line of sight $\hat{\mathbf{n}}$.

We can then write the transverse gradient inside the integral as $\nabla_\perp = \chi^{-1}\nabla_\theta$, where $\nabla_\theta \equiv (\partial_\theta, \partial_\varphi/\sin\theta)$ is the gradient on the sphere, to obtain:

$$\delta\vec{\boldsymbol{\theta}} = \nabla_\theta \Phi_L, \tag{189}$$

where we have defined the *lensing potential* Φ_L

$$\Phi_L(\hat{\mathbf{n}}, \chi_s) \equiv \int_0^{\chi_s} d\chi \, \frac{\chi_s - \chi}{\chi_s \chi}(\phi + \psi). \tag{190}$$

Since gravitational lensing typically causes displacements of at most $|\delta\vec{\boldsymbol{\theta}}| \sim 1\,\mathrm{arcmin}$, we will now proceed using the flat-sky approximation. Around the source position we define an orthogonal basis such that points around the sphere can be labelled in terms of Cartesian coordinates $\vec{\boldsymbol{\theta}} = (\theta_x, \theta_y)$. Here we will use the so-called "`HEALPix` convention", which defines the θ_x and θ_y coordinates in the directions of increasing θ and φ respectively. This is different from the IAU convention, which defines θ_x in the directon of *decreasing* θ (while θ_y is the same in both). The particular convention used to label points in the tangent space is usually a headache, since individual experiments do not always adhere to either of these two conventions exactly. In the flat-sky, we replace spherical harmonic coefficients $f_{\ell m}$ with 2D Fourier transforms:

$$f(\vec{\boldsymbol{\theta}}) = \int \frac{d\mathbf{l}^2}{(2\pi)^2} e^{i\mathbf{l}\cdot\vec{\boldsymbol{\theta}}}, \quad f_{\mathbf{l}} \equiv \int d\vec{\boldsymbol{\theta}}^2 \, f(\hat{\mathbf{n}})\, e^{-i\mathbf{l}\cdot\vec{\boldsymbol{\theta}}}. \tag{191}$$

The power spectrum of the corresponding curved-sky quantities C_ℓ^f is directly related to the Fourier-space variance in complete analogy with the 3D power spectra defined in previous sections:

$$\langle f_{\mathbf{l}} f^*_{\mathbf{l}'} \rangle = (2\pi)^2 \delta^D(\mathbf{l} - \mathbf{l}')\, C_\ell^f, \tag{192}$$

where $\ell \equiv |\mathbf{l}|^2$. The use of the flat-sky approximation here will only affect the angular derivatives, and we use it so we are not encumbered by covariant derivatives, Laplacians, Hessians etc.. This will thus only affect the ℓ-dependent prefactors that are only negligibly different from 1 [14].

The lensing displacement vector $\delta\vec{\boldsymbol{\theta}}$ is therefore the gradient of the lensing potential. In what follows we will also make use of the Hessian $H_{ij} \equiv \partial_{\theta_i}\partial_{\theta_j}\Phi_L$. We will write this 2×2 matrix as:

$$\mathsf{H} = \begin{pmatrix} \kappa + \gamma_1 & \gamma_2 \\ \gamma_2 & \kappa - \gamma_1, \end{pmatrix} \tag{193}$$

where we have defined the *convergence* κ and *shear* $\equiv(\gamma_1,\gamma_2)$ as

$$\kappa \equiv \frac{1}{2}\nabla_\theta^2\Phi_L, \quad \gamma_1 \equiv \frac{1}{2}(\partial_{\theta_x}^2 - \partial_{\theta_y}^2)\Phi_L, \quad \gamma_2 \equiv \partial_{\theta_x}\partial_{\theta_y}\Phi_L. \tag{194}$$

It is common to bundle up the two components of the displacement into a single complex number:

$$\alpha \equiv \delta\theta_x + i\delta\theta_y, \tag{195}$$

and to do the same thing with the two shear components:

$$\gamma \equiv \gamma_1 + i\gamma_2. \tag{196}$$

The resulting quantities quantities then respond to rotations of the local flat coordinate system by an angle β as

$$\alpha \to \alpha e^{i\beta}, \quad \gamma \to \gamma e^{i2\beta}. \tag{197}$$

This is simply a manifestation of the fact that the fields α and γ are spin-1 and spin-2 irreducible representations of the $U(1)/SO(2)$ group.

Now let us define the following two combinations of the Fourier components of γ (the so-called E-mode and B-mode components):

$$E_{\mathbf{l}} \equiv \gamma_{1,\mathbf{l}}\frac{l_x^2-l_y^2}{l_x^2+l_y^2} + \gamma_{2,\mathbf{l}}\frac{2l_xl_y}{l_x^2+l_y^2}, \quad B_{\mathbf{l}} \equiv -\gamma_{1,\mathbf{l}}\frac{2l_xl_y}{l_x^2+l_y^2} + \gamma_{2,\mathbf{l}}\frac{l_x^2-l_y^2}{l_x^2+l_y^2}. \tag{198}$$

It is straightforward to show that there is a direct correspondence between the shear E-mode and the convergence κ, and that the B-mode should be zero:

$$E_{\mathbf{l}} = \kappa_{\mathbf{l}}, \quad B_{\mathbf{l}} = 0. \tag{199}$$

Thus, a map of γ can always be converted into κ.

Finally, we can relate κ to the matter overdensity δ. To do so, we pull the angular Laplacian defining κ into the radial integral, and transform it back into the 3D Laplacian as $\nabla_\theta^2 = \chi^2(\nabla^2 - \partial_\chi^2)$. The radial derivative component can be cancelled out after integrating Eq. 190 by parts. The result can then be related to δ assuming $\psi = \phi$, and using Poisson's equation (Eq. 42). The result is:

$$\kappa(\hat{\mathbf{n}},\chi_s) = \frac{3}{2}H_0^2\Omega_m\int_0^{\chi_s} d\chi\,\frac{\chi}{a(\chi)}\,\frac{\chi_s-\chi}{\chi_s}\,\delta(\chi\hat{\mathbf{n}},\eta). \tag{200}$$

6.2 Galaxy weak lensing

Through its perturbation of the photon trajectories, gravitational lensing will distort the observed shapes of galaxies in a coherent way. By correlating the shapes of these galaxies we can therefore statistically study the properties of the matter distribution.

Let $I(\vec{\boldsymbol{\theta}})$ be the observed intensity (flux per solid angle) from a galaxy. Because lensing preserves intensity (it only moves photons around, but does not create more of them),

$$I(\vec{\boldsymbol{\theta}}) = I_u(\vec{\boldsymbol{\theta}}_u), \tag{201}$$

where $I_u(\vec{\boldsymbol{\theta}}_u)$ is the true intensity (in the absence of lensing), evaluated at the unlensed angular coordinates. From Eq. 189, the unlensed and observed coordinates are related by:

$$\vec{\boldsymbol{\theta}} = \vec{\boldsymbol{\theta}}_u + \nabla_\theta\Phi_L. \tag{202}$$

Let $\vec{\boldsymbol{\theta}}_0$ and $\vec{\boldsymbol{\theta}}_{u,0}$ be the angular position of the galaxy's centre in both coordinates, and let us define the displacements from this centre: $\Delta\vec{\boldsymbol{\theta}} \equiv \vec{\boldsymbol{\theta}} - \vec{\boldsymbol{\theta}}_0$, and $\Delta\vec{\boldsymbol{\theta}}_u \equiv \vec{\boldsymbol{\theta}}_u - \vec{\boldsymbol{\theta}}_{u,0}$. Expanding $\nabla_\theta\Phi_L$, the relation between displacements in the observed and true coordinates are given by

$$\Delta\vec{\boldsymbol{\theta}} = (\mathbb{1} + \mathsf{H})\;\Delta\vec{\boldsymbol{\theta}}_u. \tag{203}$$

With this, the galaxy flux is given by:

$$F = \int d^2\vec{\boldsymbol{\theta}}\, I(\vec{\boldsymbol{\theta}}) = \det(\mathbb{1} + \mathsf{H}) \int d^2\vec{\boldsymbol{\theta}}_u\, I_u(\vec{\boldsymbol{\theta}}_u) = (1 + 2\kappa) F_u, \tag{204}$$

where F_u is the unlensed flux, and we have only kept terms to lowest order in H. Note that we pull $\mathbb{1} + \mathsf{H}$ out of the integral under the assumption that gravitational lensing varies over scales ($\sim$ arcmin) larger than the scale over which the galaxy image varies ($\sim$ arcsec.).

To characterise the shape of the galaxy, we define the galaxy's inertia tensor as

$$q^{ij} = \frac{1}{F} = \int d^2\vec{\boldsymbol{\theta}}\, I(\hat{\mathbf{n}}) \Delta\theta^i \Delta\theta^j. \tag{205}$$

It will be useful to split q into its trace and its traceless components:

$$\mathsf{q} = \frac{Q}{2} \begin{pmatrix} 1 + \varepsilon_1 & \varepsilon_2 \\ \varepsilon_2 & 1 - \varepsilon_1 \end{pmatrix}. \tag{206}$$

Here, $Q \equiv \mathrm{Tr}(\mathsf{q})$ is a measure of the source area, while $(\varepsilon_1, \varepsilon_2)$ parametrize the galaxy ellipticity. As before, transforming the integral defining q to the unlensed coordinates, we obtain, to lowest order in H:

$$\mathsf{q} = \mathsf{q}_u + \mathsf{q}_u\, \mathsf{H} + \mathsf{H}\, \mathsf{q}_u. \tag{207}$$

This leads to the following relation between the lensed and unlensed areas and ellipticities:

$$Q = Q_u(1 + 2\kappa) + Q_N, \quad \varepsilon_i = 2\gamma_i + \varepsilon_{N,i}, \tag{208}$$

where the noise components Q_N, ε_N are

$$Q_N = Q_u \delta_N, \quad \varepsilon_{N,i} = \varepsilon_{u,i}(1 - \delta_N), \quad \delta_N \equiv 2(\varepsilon_{u,1}\gamma_1 + \varepsilon_{u,2}\gamma_2). \tag{209}$$

The terms proportional to δ_N are often neglected. If the true ellipticities are uncorrelated, they are simply an additional noise-like contribution. If the true ellipticities are partially correlated (e.g. through intrinsic alignments), these term are of the same order (second) as several other terms we have so far discarded.

Hence, galaxy ellipticities receive a coherent contribution from lensing of the form 2γ, which can be mapped by effectively averaging over many galaxies. In deriving this, we have also uncovered two more effects: the apparent source area and the observed flux both receive a correction of the form $1 + 2\kappa$. In both cases, this is caused by a perturbation to the angular diameter distance (or luminosity distance) of the form $1 + \kappa$. This effect is known as *magnification*, and can in fact be detected from the observed clustering of galaxies. The modification to the angular diameter distance perturbs the observed angular positions of galaxies, diluting their density in the presence of matter overdensities along the line of sight. On the other hand, the corresponding positive modification to the observed source flux also causes galaxies beyond the sample flux limit to be detected, increasing the observed overdensity. These two effects lead to an overall effective contribution to the overdensity of galaxies, labelled *magnification bias*, and given by

$$\delta_g^\mu = (5s - 2)\kappa, \tag{210}$$

where $s \equiv d\log_{10} N/dm$ is the logarithmic slope of the sample number counts with respect to apparent magnitude at the flux limit.

6.3 CMB lensing

Gravitational lensing also modifies the trajectories of CMB photons, thus affecting the properties of the observed temperature anisotropies. Since gravitational lensing does not modify intensity, the impact of lensing is second-order in perturbations. The effect, however, is larger than other second-order contributions, and can be detected to very high significance in CMB data.

Since intensity is conserved, lensing simply reshuffles the observed photon angular coordinates. The lensed and unlensed temperature fluctuations are thus related to one another via:

$$\delta T(\vec{\boldsymbol{\theta}}) = \delta T_u(\vec{\boldsymbol{\theta}} - \delta\vec{\boldsymbol{\theta}}) \simeq \delta T_u(\vec{\boldsymbol{\theta}}) - \nabla_\theta \Phi_L(\vec{\boldsymbol{\theta}}) \cdot \nabla_\theta \delta T_u(\vec{\boldsymbol{\theta}}). \tag{211}$$

In Fourier space this reads:

$$\delta T_{\mathbf{l}} = \delta T_{u,\mathbf{l}} + \int \frac{d^2\mathbf{l}'}{(2\pi)^2} \mathbf{l}' \cdot (\mathbf{l} - \mathbf{l}')\, \Phi_{L,\mathbf{l}'}\, \delta T_{u,\mathbf{l}-\mathbf{l}'}. \tag{212}$$

Since the lensing potential is mostly caused by the large-scale structure at low redshifts ($z \lesssim 10$), Φ_L is to a good approximation uncorrelated with δT_u. In this sense, the second term in Eq. 211 can be interpreted, for a fixed Φ_L as breaking the statistical isotropy of the unlensed temperature fluctuations. As such, lensing will induce correlations between different Fourier modes and these can be used to reconstruct the lensing potential. Consider the correlator of two lensed temperature modes with different angular wave vectors $\mathbf{l} \neq \mathbf{l}'$ for a fixed lensing potential, and expand it to lowest order int Φ_L

$$\langle \delta T_{\mathbf{l}} \delta T^*_{\mathbf{l}'} \rangle_{\Phi_L} = \Phi_{L,\mathbf{l}-\mathbf{l}'}\, (\mathbf{l} - \mathbf{l}') \cdot (\mathbf{l} C^T_\ell - \mathbf{l}' C^T_{\ell'}),$$

where $\langle \cdots \rangle_{\Phi_L}$ indicates ensemble averaging keeping Φ_L constant.

Thus, for a given mode $\mathbf{L}$, $\Phi_{L,\mathbf{L}}$ can be estimated by combining products of lensed temperature modes $\delta T_{\mathbf{l}} \delta T^*_{\mathbf{l}'}$ such that $\mathbf{l} - \mathbf{l}' = \mathbf{L}$, i.e.:

$$\hat{\Phi}_{L,\mathbf{L}} = \int \frac{d^2\mathbf{l}}{(2\pi)^2} \delta T_{\mathbf{l}}\, \delta T_{\mathbf{l}-\mathbf{L}}\, g(\mathbf{l}, \mathbf{L}). \tag{213}$$

This is the so called *quadratic estimator* for lensing reconstruction. The optimal kernel $g(\mathbf{l}, \mathbf{L})$ can be found by minimising the variance of the resulting lensing potential map (see [13]).

Lensing reconstruction allows us to obtain maps of the lensing convergence at the surface of last scattering. As shown in Eq. 200, such a map contains information about the matter density fluctuations integrated along the line of sight from $z = 1100$, and thus can be used to study the growth history from the moment of recombination. This is particularly powerful in cross-correlation with other tracers of the matter fluctuations at specific redshifts, allowing us to easily recover the redshift dependence of structure growth, which is an invaluable tool to study the nature of dark energy and modified gravity.

References

[1] V. Mukhanov, *Physical Foundations of Cosmology*. Cambridge Univ. Press, Cambridge, 2005. https://cds.cern.ch/record/991646.

[2] S. Dodelson, *Modern cosmology*. Academic Press, San Diego, CA, 2003. https://cds.cern.ch/record/1282338.

[3] D. Baumann, *Cosmology lecture notes*. http://cosmology.amsterdam/education/cosmology/.

[4] S. Weinberg, *Cosmology*. 2008.

[5] S. Weinberg, *Gravitation and Cosmology: Principles and Applications of the General Theory of Relativity*. Wiley, New York, NY, 1972. https://cds.cern.ch/record/100595.

[6] H. Mo, F. C. van den Bosch, and S. White, *Galaxy Formation and Evolution*. 2010.

[7] J. A. Peacock, *Cosmological Physics*. Cambridge University Press, 1999.

[8] F. Bernardeau, S. Colombi, E. Gaztanaga, and R. Scoccimarro, "Large scale structure of the universe and cosmological perturbation theory," *Phys. Rept.* **367** (2002) 1–248, arXiv:astro-ph/0112551.

[9] R. Durrer, *The Cosmic Microwave Background*. Cambridge University Press, 2008.

[10] C.-P. Ma and E. Bertschinger, "Cosmological perturbation theory in the synchronous and conformal Newtonian gauges," *Astrophys. J.* **455** (1995) 7–25, arXiv:astro-ph/9506072.

[11] A. R. Liddle and D. H. Lyth, *Cosmological Inflation and Large-Scale Structure*. Cambridge Univ. Press, Cambridge, 2000. https://cds.cern.ch/record/452061.

[12] M. Bartelmann and P. Schneider, "Weak gravitational lensing," *Phys. Rept.* **340** (2001) 291–472, arXiv:astro-ph/9912508.

[13] A. Lewis and A. Challinor, "Weak gravitational lensing of the CMB," *Phys. Rept.* **429** (2006) 1–65, arXiv:astro-ph/0601594.

[14] M. Kilbinger *et al.*, "Precision calculations of the cosmic shear power spectrum projection," *Mon. Not. Roy. Astron. Soc.* **472** no. 2, (2017) 2126–2141, arXiv:1702.05301 [astro-ph.CO].

A Problems

Problem 1: Photon geodesics

The trajectory and energy of a photon propagating through the Universe will be affected by perturbations in the metric. For a perturbed FRW in conformal coordinates, and using the Newtonian gauge, i.e.

$$d\tau^2 = a^2(\eta)\,\left[(1+2\psi)d\eta^2 - (1-2\phi)|d\mathbf{x}|^2\right], \tag{214}$$

show that the redshift of a photon propagating from a source with velocity $\mathbf{v}_s$ to an observer with velocity $\mathbf{v}_0$ is given by

$$1+z = \frac{1}{a}\left[1-\psi+\psi_0+\hat{\mathbf{n}}\cdot(\mathbf{v}_s-\mathbf{v}_0)+\int_{\eta_0}^{\eta} d\eta'\,(\phi'+\psi')\right], \tag{215}$$

where $\hat{\mathbf{n}}$ is a unit vector along the line of sight, and the subscript $_0$ denotes quantities evaluated at the observer. What is the physical interpretation of the different terms entering this equation?

Show also that the photon follows a trajectory

$$\mathbf{x}(\eta) = \hat{\mathbf{n}}\int_{\eta}^{\eta_0} d\eta'\,(1+\phi+\psi) - \int_{\eta}^{\eta_0} d\eta'(\eta'-\eta)\nabla_\perp(\phi+\psi). \tag{216}$$

Hints:

- Start by writing down the geodesic equation for the photon 4-momentum $p^\mu = dx^\mu/d\lambda$:

$$\frac{dp^\mu}{d\lambda} + \Gamma^\mu_{\nu\sigma}p^\nu p^\sigma = 0, \tag{217}$$

  as well as the null condition

$$p^\mu p^\nu g_{\mu\nu} = 0 \tag{218}$$

  to first order in the perturbations.

- Change variables to the directional vector $\hat{\mathbf{e}} \equiv \mathbf{p}/|\mathbf{p}|^2$, and the comoving energy $\epsilon \equiv a\,p_\mu u_c^\mu$, where $u_c^\mu = a^{-1}(1-\psi)\delta_0^\mu$ is the 4-velocity of an observer with constant comoving coordinates (why?). Integrate the resulting two equations to find $\epsilon(\eta)$ and $\mathbf{x}(\eta)$ along the photon trajectory.

- Noting that the frequency measured by an observer with 4-velocity u^μ is $h_P\nu = p^\mu u_\mu$, write the 4-velocity of source and observer as $u_q^\mu = a^{-1}(1-\psi,\mathbf{v})$ (why?), and use the equation for ϵ to obtain Eq. 215, where the redshift is defined as $1+z \equiv (u_s^\mu p_\mu)/(u_0^\mu p_\mu)$.

Problem 2: Perturbations during radiation domination

In the lectures we showed that the Newtonian potential ψ stays constant during matter domination. Let's now examine the solution during radiation domination. Solve Einstein's equations in the Newtonian gauge during radiation domination to show that the gravitational potential evolves as

$$\psi(k,\eta) \propto \frac{j_1(c_s k\eta)}{c_s k\eta}, \tag{219}$$

where $c_s = 1/\sqrt{3}$ is the sound speed for radiation, and $j_1(x)$ is the spherical Bessel function of the first kind:

$$j_1(x) = \frac{\sin x - x\cos x}{x^2}. \tag{220}$$

What is the behaviour on super-horizon and sub-horizon scales?

Hints:

- Recall Einstein's equations for a perfect fluid in the Newtonian gauge:

$$k^2\psi + 3\mathcal{H}(\psi' + \mathcal{H}\psi) = -4\pi G a^2\,\bar{\rho}\,\delta, \tag{221}$$

$$k^2(\psi' + \mathcal{H}\psi) = 4\pi G a^2\,(\bar{\rho} + \bar{p})\theta, \tag{222}$$

$$\psi'' + 3\mathcal{H}\psi' + (2\mathcal{H}' + \mathcal{H}^2)\psi = 4\pi G a^2\, c_s^2\bar{\rho}\,\delta. \tag{223}$$

  Combine two of these to write an equation involving ψ alone.

- Use the fact that $a \propto t^{1/2} \propto \eta$ during radiation domination to simplify this equation.

- Solve the resulting equation by noting that the spherical Bessel functions satisfy the equation

$$x^2 j_n'' + 2x j_n' + (x^2 - n(n+1))j_n = 0. \tag{224}$$

Problem 3: Curvature perturbations

In the lectures we argued that ψ stays constant on super-horizon scales as long as the equation of state doesn't vary. Show that the following quantity (the "curvature perturbation") does stay constant even if the equation of state varies:

$$\mathcal{R} \equiv -\phi - \frac{\mathcal{H}(\psi' + \mathcal{H}\phi)}{4\pi G a^2(\bar{\rho} + \bar{p})}. \tag{225}$$

Hints:

- Use Einstein's equations (Eqs. 221-223) to write $\mathcal{R}$ in terms of ϕ and δ alone, on super-horizon scales ($k \ll \mathcal{H}$), as

$$\mathcal{R} \simeq -\phi - \frac{\bar{\rho}\delta}{3(\bar{\rho} + \bar{p})}. \tag{226}$$

- Remember that the continuity equation reads:

$$\delta' = -(1+w)(\theta - 3\phi') - 3\mathcal{H}(c_s^2 - w)\delta. \tag{227}$$

  Show that the term involving θ can be dropped (why?), and use Eq. 226 to replace ψ with $\mathcal{R}$. This gives you an ODE for $\mathcal{R}$.

- Use the continuity equation for the background ($\bar{\rho}' = -3\mathcal{H}(\bar{\rho} + \bar{p})$) to simplify this equation, and show that

$$\mathcal{R}' = -\frac{\mathcal{H}\bar{\rho}}{\bar{\rho} + \bar{p}} \left(\frac{\delta p}{\bar{\rho}} - \frac{\bar{p}'}{\bar{\rho}'} \delta \right). \tag{228}$$

  Can we say that the right hand side is zero, thus proving what we wanted?

Problem 4: From 3D to 2D.

Consider a quantity defined on the sphere $f(\hat{\mathbf{n}})$ in terms of a radial lightcone integral over a three-dimensional quantity $F(\mathbf{x}, \eta)$:

$$f(\hat{\mathbf{n}}) = \int^{\eta_0} d\eta \, q_f(\chi) F(\chi \hat{\mathbf{n}}, \eta), \tag{229}$$

where $q_f(\chi)$ is a radial kernel. Assume now that the three-dimensional quantity is linearly related to the primordial curvature perturbation $\mathcal{R}_{\mathbf{k}}$ through a transfer function $T_F(k, \eta)$:

$$F_{\mathbf{k}}(\eta) = T_F(k, \eta) \, \mathcal{R}_{\mathbf{k}}. \tag{230}$$

Show that the harmonic coefficients of f are then related to $\mathcal{R}_{\mathbf{k}}$ through:

$$f_{\ell m} = \int \frac{dk}{2\pi^2} k^2 \, \Delta^f_\ell(k) i^\ell \int d\hat{\mathbf{n}}_{\mathbf{k}} \, Y^*_{\ell m}(\hat{\mathbf{n}}_{\mathbf{k}}) \, \mathcal{R}_{\mathbf{k}}, \tag{231}$$

where $\hat{\mathbf{n}}_{\mathbf{k}} \equiv \mathbf{k}/k$, and

$$\Delta^f_\ell(k) = \int d\chi \, q_v(\chi) \, T_F(k, \eta) \, j_\ell(k\chi). \tag{232}$$

Then, show that the angular power spectrum of f is related to the primordial power spectrum $\Delta^2_{\mathcal{R}}(k)$ through

$$C^f_\ell = \frac{2}{\pi} \int \frac{dk}{k} \, |\Delta^f_\ell(k)|^2 \, \Delta^2_{\mathcal{R}}(k). \tag{233}$$

Hints:

- Use the plane-wave expansion to relate the harmonic coefficients of f to the Fourier coefficients of F:

$$e^{i\mathbf{k}\cdot\mathbf{x}} = 4\pi \sum_{\ell m} i^\ell \, j_\ell(k\chi) \, Y_{\ell m}(\hat{\mathbf{n}}) \, Y^*_{\ell m}(\hat{\mathbf{n}}_{\mathbf{k}}), \tag{234}$$

  where $j_\ell(x)$ is the spherical Bessel function of order ℓ.

- Remember the definition of the primordial power spectrum

$$\langle \mathcal{R}^*_{\mathbf{k}} \mathcal{R}_{\mathbf{k}'} \rangle \equiv \frac{2\pi^2}{k^3} \Delta^2_{\mathcal{R}}(k) \, (2\pi)^3 \delta^D(\mathbf{k} - \mathbf{k}'). \tag{235}$$

Problem 5: The growth factor

The evolution equation for the overdensity of non-relativistic, pressureless matter, neglecting all perturbations in any other species can be written, in the Newtonian limit, as:

$$\ddot{\delta} + 2H\dot{\delta} - 4\pi G\rho_M(t)\,\delta = 0,$$

where $H = \dot{a}/a$ is the expansion rate and ρ_M is the non-relativistic matter density.

1. Change the time variable from t to a to change the form of this equation to:

$$\delta'' + \left(\frac{H'}{H} + \frac{3}{a}\right)\delta' - \frac{3}{2}\frac{H_0^2\Omega_M}{H^2\,a^5}\delta = 0, \tag{236}$$

   where $f' \equiv df/da$ and Ω_M and H_0 are the matter parameter and expansion rate today.

2. Show that, for a matter dominated universe, a possible solution to this equation is $\delta_1 = H$. For this you'll need to use the fact that in this case $H^2 \simeq H_0^2\Omega_M/a^3$. Is this a growing-mode solution?

3. Consider the more general case where $H^2 = H_0^2\left(\Omega_M/a^3 + \sum_i \Omega_i\, a^{-3(1+w_i)}\right)$. For what values of the equation of state parameter w_i is $\delta_1 = H$ still a solution? What components do these values correspond to?

4. For a second-order equation with two independent solutions δ_1 and δ_2 the Wronskian W is defined as $W \equiv \delta_1'\delta_2 - \delta_1\delta_2'$. Prove that for equation 236 the Wronskian satisfies

$$\frac{W'}{W} = -\left(\frac{H'}{H} + \frac{3}{a}\right). \tag{237}$$

   Integrate this equation to show that $W = C/(a^3\,H)$, where C is an integration constant.

5. Using the previous result and under the ansatz $\delta_2(a) = \delta_1(a)\,g(a)$ prove that the second solution is

$$\delta_2 = -C\,H(a)\int_0^a \frac{da'}{[a'\,H(a')]^3}. \tag{238}$$

6. We know that at early times ($a << 1$), during matter domination, $\delta = a$. Find the value of the integration constant C that gives this normalization.